Accepted Manuscript

Design and synthesis of thienopyrimidine urea derivatives with potential cytotoxic and pro-apoptotic activity against breast cancer cell line MCF-7

Eman F. Abdelhaleem, Mohammed K. Abdelhameid, Asmaa E. Kassab, Manal M. Kandeel

PII: S0223-5234(17)30877-2

DOI: 10.1016/j.ejmech.2017.10.075

Reference: EJMECH 9867

To appear in: *European Journal of Medicinal Chemistry*

Received Date: 5 July 2017

Revised Date: 28 September 2017

Accepted Date: 28 October 2017

Please cite this article as: E.F. Abdelhaleem, M.K. Abdelhameid, A.E. Kassab, M.M. Kandeel, Design and synthesis of thienopyrimidine urea derivatives with potential cytotoxic and pro-apoptotic activity against breast cancer cell line MCF-7, *European Journal of Medicinal Chemistry* (2017), doi: 10.1016/j.ejmech.2017.10.075.

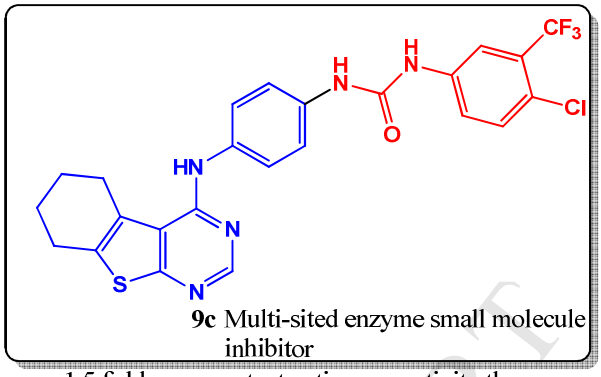

9c Multi-sited enzyme small molecule inhibitor

Orthogonal 4-anilino-thienopyrimidine head

IC_{50} VEGFR-2 = 0.20 μM. ⇐

Substituted phenyl urea tail

1.5 folds more potent anticancer activity than doxorubicin against MCF-7.

⇓ Coplanar polycyclic head

Acceptor-donor pair hydrogen bond tail

IC_{50} topoisomerase II = 9.29 μM.

⇓

Cell cycle arrest at G2/M phase.
Increase p53 level.
Elevation in Bax/ BCL-2 ratio.
Increase in the level of active caspase-3

} Intrinsic mitochondrial pathway of apoptosis.

Design and Synthesis of Thienopyrimidine Urea Derivatives with Potential Cytotoxic and Pro-apoptotic Activity against Breast Cancer Cell Line MCF-7

Eman F. Abdelhaleem[a], Mohammed K. Abdelhameid [a], Asmaa E. Kassab [a], Manal M. Kandeel [b].

[a] Pharmaceutical Organic Chemistry Department, Faculty of Pharmacy, Cairo University, Cairo 11562, Egypt.

[b] Pharmaceutical Chemistry Department, Faculty of Pharmaceutical Sciences and Pharmaceutical Industries, Future University, Cairo 12311, Egypt.

Address: 33 Kasr El-Aini Street, Cairo, Egypt.

Design and Synthesis of Thienopyrimidine Urea Derivatives with Potential Cytotoxic and Pro-apoptotic Activity against Breast Cancer Cell Line MCF-7

Correspondence to: Asmaa E. Kassab, Pharmaceutical Organic Chemistry Department, Faculty of Pharmacy, Cairo University, Cairo 11562, Egypt.

Tel: 002023639307.

Fax: 002023635140.

E-mail: asmaa.kassab@pharma.cu.edu.eg

Abstract

A series of novel tetrahydrobenzothieno[2,3-d]pyrimidine urea derivatives was synthesized according to fragment-based design strategy. They were evaluated for their anticancer activity against MCF-7 cell line. Three compounds **9c**, **9d** and **11b** showed 1.5-1.03 folds more potent anticancer activity than doxorubicin. In this study, a promising multi-sited enzyme small molecule inhibitor **9c**, which showed the most potent anti-proliferative activity, was identified. The anti-proliferative activity of this compound appears to correlate well with its ability to inhibit topoisomerase II (IC_{50}= 9.29 µM). Moreover, compound **9c** showed excellent VEGFR-2 inhibitory activity, at the sub-micromolar level with IC_{50} value 0.2 µM, which is 2.1 folds more potent than sorafenib. Moreover, activation of damage response pathway of the DNA leads to cell cycle arrest at G2/M phase, accumulation of cells in pre-G1 phase and annexin-V and propidium iodide staining, indicating that cell death proceeds through an apoptotic mechanism. Compound **9c** showed potent pro-apoptotic effect through induction of the intrinsic mitochondrial pathway of apoptosis. This mechanistic pathway was confirmed by a significant increase in the expression of the tumor suppressor gene p53, elevation in Bax/ BCL-2 ratio and a significant increase in the level of active caspase-3. Quantitative structure-activity relationship (QSAR) studies delivered equations of five 3D descriptors with R^2 = 0.814. This QSAR model provides an effective technique for understanding the observed antitumor properties and thus could be adopted for developing effective lead structures.

Key words: Thieno[2,3-d]pyrimidines; Aryl urea; Fragment-based Design; Synthesis; Anticancer activity; Topoisomerase II; VEGFR-2; Cell cycle arrest profile; Apoptosis; QSAR.

1. Introduction

Cancer is a major health problem worldwide. Among the various types of malignant tumors, breast cancer is the second leading cause of death in women [1]. In advanced solid tumor including breast cancer, tumor growth and metastasis has been linked to overexpression of DNA topoisomerase (topo) enzymes and pathological angiogenesis via vascular endothelial growth factor (VEGFR) pathway [2]. Topoisomerases are a family of enzymes that control DNA synthesis, modulators of topo are now widely used as cytotoxic agents [3], this class of drugs acts either by topo poisoning via interchelation with DNA as doxorubicin and amsacrine (figure 1) or acts as catalytic inhibitors as TSC24 (figure 1) [4]. The common structural basis for the action of these drugs is linear or curved polycyclic core bearing a flexible side chain that anchors DNA by hydrogen bond formation [5]. As a catalytic topo inhibitor, TSC24 acts by blocking the ATP-binding site of the enzyme leading to inactivation of enzyme [6]. Topo modulators are efficient; however, they produce detrimental secondary effects [5]. Therefore, it would be useful to design newer products, such as aroylthiourea derivative **I** (figure 1), which will be more potent and better tolerated, being able to interfere with both topo and tyrosine kinases [7, 8]. This dual activity increases cytotoxic properties of the compound and decreases its side effects. Activation of the DNA damage response pathway leads, in most cases, to drug-induced apoptosis and/or to cell cycle arrest in G1, S, and G2 phases [9]. Vascular Endothelial Growth Factor Receptor-2 (VEGFR-2), also known as Kinase

Insert Domain Receptor (KDR), is a Receptor Tyrosine Kinase and is one of the major regulators of both physiologic and pathologic angiogenesis. Therapies based on targeted antiangiogenic agents, such as sorafenib (figure 2), are supposed to be less toxic than conventional chemotherapy [10] and, when used in combination with doxorubicin, increases potency of chemotherapy [11]. Sorafenib is structurally a member of diaryl urea family that act as (Receptor Tyrosine Kinase) RTK inhibitors, especially as VEGFR-2 inhibitors, and induces apoptosis of cancer cells [12]. Other members of this family are, a p38 inhibitor (doramapimod), compounds **II** and **III** are VEFGR-2 inhibitors (figure 2). Compound **II** is with substituted thienopyrimidine heterocyclic core, while compound **III** is a quinoline derivative. The main structural features of this urea family are head group formed from orthogonal polycyclic ring that bind to adenine region of ATP and phenyl urea tail that bind to allosteric site of kinase enzyme [13]. The therapeutic chemotherapy protocol must be balanced in terms of therapeutic effectiveness and minimization of treatment-associated side effects. Multi-sited enzyme small molecule inhibitors are now one of the potential fields in cancer drug discovery to reach the same therapeutic goal. One of the used approaches to obtain such multi-sited enzyme inhibitors is fragment-based lead generation. Fragments are scaffolds that usually form part of drugs that are responsible of biological activities. These fragments are then combined to generate lead compounds [14]. Based on a structural analysis of the topo and VEGFR-2 inhibitors, we have constructed a 'hybrid-design' model (figure 3) with topo and VEGFR-2 inhibitors structural features. We have used polycyclic fused tetrahydrobenzothienopyrimidine, as large coplanar core, or orthogonal ring with aniline moiety, as head part that satisfies ATP domain of both enzymes, attached to aryl urea as tail part that can anchor DNA or interacts with the binding site of both enzymes, as

antagonists with some structural modification in the head or tail group (figure 3). In the current study, all target compounds were evaluated for their anti-proliferative activity *in vitro* against MCF-7 cell line. In order to explore the mechanistic pathways of the anticancer activity of the synthesized compounds, we chose the most potent compound **9c** to perform extra investigations such as cell cycle analysis, topoisomerase II, and VEGFR-2 assays and apoptosis markers. In this work, quantitative structure-activity relationship (QSAR) studies were also performed, for validating the observed antitumor properties.

2. Results and discussion

2. 1. Chemistry

The synthesis of the target compounds is outlined in Schemes **1** -**3**. Our primary starting material 4-chloro-5,6,7,8-tetrahydrobenzo[4,5]thieno[2,3-d]pyrimidine (**1**) [15] reacted with hydrazine hydrate to afford **2** [15]. Reacting with the appropriate isocyanates in methylene chloride, the 4-hydrazinyl-5,6,7,8-tetrahydrobenzo[4,5]thieno[2,3-d]pyrimidine (**2**) gave the thienopyrimidine urea derivatives **3a-e**. The ^{1}H NMR spectra of **3a-e** displayed the presence of signals at δ 7.12-8.13 ppm, corresponding to different NH-Ar groups which were not present in **2**. On the other hand, ^{13}C NMR spectra of compounds **3b** & **3d** revealed the appearance of (C=O) carbon at δ 166.07 and 155.98 ppm, respectively. In the present study, hoping to synthesize the triazolothienopyrimidine **5**, the chlorothienopyrimidine **1** was allowed to react with thiosemicarbazide in ethanol. Actually, unexpected hydrazinecarbothioamide derivative **4** was obtained after heating under reflux for 8 h. The IR spectrum of compound **4** indicated the presence of three absorption bands at the range 3417-3147 cm^{-1} , due to two NH and NH_2 groups, in addition to the C=S group that

appeared as an absorption band at 1292 cm^{-1}. Further evidence was obtained from the ^{1}H NMR spectrum that showed four exchangeable signals at δ 7.67, 7.77, 8.63 and 9.29 ppm assigned to NH_2 and two NH protons. Further structural evidence stemmed from the ^{13}C NMR spectrum of compound **4** that revealed the presence of (C=S) carbon at δ 182.23 ppm. In the present study, compound **5** was prepared by reacting the 4-chlorothienopyrimidine derivative **1** with thiosemicarbazide in ethanol and extending the reflux time to 20 h. The IR spectrum of **5** lacked the presence of C=S group, which confirmed the success of cyclization. The ^{1}H NMR spectrum showed only one exchangeable signal at δ 6.45 ppm due to NH_2 protons. Reacting the triazolothienopyrimidine derivative **5** with the appropriate isocyanates afforded **6a-c**. ^{1}H NMR spectra of these compounds displayed the characteristic signals corresponding to different NH-Ar groups. The ^{13}C NMR spectra of compounds **6a** & **6b** revealed the appearance of signals due to (C=O) carbon at δ 167.10 and 167.08 ppm, respectively. The triazolothienopyrimidine derivatives **7a,b** were achieved by the reaction of compound **5** with the appropriate isothiocyanates. The ^{1}H NMR spectra of **7a,b** displayed the presence of the characteristic signals of aromatic protons at δ 7.13-7.65 ppm. In addition, the ^{13}C NMR spectrum of compound **7a** showed the appearance of signal at δ 174.60 ppm corresponding to (C=S) carbon. The thienopyrimidine diarylurea derivatives **9a-e** were obtained by reacting the thienopyrimidine **8** [16] with the appropriate isocyanates in methylene chloride. The ^{1}H NMR spectra of **9a-e** showed the appearance of three exchangeable singlet signals at δ 7.78-9.52 ppm corresponding to three NH protons, in addition to the expected signals corresponding to different NH-Ar protons. The ^{13}C NMR spectra of compounds **9b** & **9e** revealed the appearance of (C=O) carbon at δ 165.96 & 165.49 ppm, sequentially. Reacting

compound **9b** or **9d** and 4-bromophenacyl bromide in ethanol afforded compounds **10a,b**. The ^{1}H NMR spectra of these derivatives revealed the disappearance of the signals due to two NH protons. Moreover, ^{13}C NMR spectra showed the disappearance of the signal corresponding to (C=O) carbons. The synthesis of compounds **11a-g** was accomplished through reacting the thienopyrimidine derivative **8** with the appropriate isothiocyanates. The ^{1}H NMR spectra of **11a-g** showed the presence of three exchangeable singlet signals at δ 7.96-10.74 ppm, corresponding to three NH protons. The ^{13}C NMR spectra of compounds **11a** & **11b** showed the appearance of signals at δ 172.47 & 172.46 ppm, respectively, corresponding to (C=S) carbon. Cyclization of compounds **11a** or **11e** with 4-bromophenacyl bromide resulted in the formation of compounds **12a,b**. The ^{1}H NMR spectra of these derivatives lacked the presence of the two exchangeable singlet signals due to the two NH protons. Compound **14** was obtained in a good yield through reacting the 2-choromethyl derivative **13** [17] with *p*-phenylene diamine in ethanol in the presence of catalytic amount of triethylamine. The ^{1}H NMR spectrum of **14** showed additional two exchangeable signals at δ 8.28 and 5.75 ppm, due to NH and NH_2 protons of 2-aryl amino methyl group, which were not present in the starting chloromethyl derivative **13**, in addition to the signals at δ 6.61-7.36 ppm, corresponding to the aromatic protons. Finally, compound **14** was reacted with the appropriate isothiocyanates to give **15a-e**. The ^{1}H NMR spectra of **15a-e** displayed four exchangeable signals at δ 7.67-12.18 ppm, assigned to four NH protons. On the other hand, the ^{13}C NMR spectra of compounds **15d** & **15e** showed the appearance of signals at δ 180.08 & 180.66 ppm, respectively corresponding to (C=S) carbons.

2. 2. *In vitro* anticancer activity

The anticancer activity of the newly synthesized compounds was examined against MCF-7 cell line compared to doxorubicin as reference anticancer drug. The results of the mean values of experiments performed in triplicate, expressed as half maximal inhibitory concentration (IC_{50}) values, were summarized in Tables 1-3 and presented graphically in figures 4 and 5. The *in vitro* results showed that most of the test compounds showed moderate to significant antitumor activity against MCF-7 cell line. Three compounds **9c**, **9d** and **11b** showed 1.5-1.03 folds more potent anticancer activity than doxorubicin. Three compounds **3d**, **3e** and **6a** showed anticancer activity comparable to doxorubicin with IC_{50} values 28.02, 22.65 and 29.06 μM, respectively. Compounds **3c**, **9b**, **9e**, **11a**, **11c-f** and **12a** showed moderate anticancer activity. The antitumor activity correlation of the newly synthesized compounds showed that among the diaryl urea and thiourea derivatives compounds **9c**, **9d** and **11b**, bearing electron withdrawing groups, showed more potent anticancer activity than the other unsubstituted and substituted derivatives with electron donating groups and were found to be more potent than doxorubicin. Moreover, compounds **9c** and **11b** bearing electron withdrawing group at *p*-position were found to be more potent than compound **9d**. Another interesting phenomenon is that introducing two groups into the 2 and 6 positions of the terminal phenyl ring in compounds **9a**, **9b** and **11c** resulted in lower anticancer activity. Replacement of the orthogonal 4-anilinothienopyrimidine head with pseudo tetracyclic core with movement of the diaryl urea tail to position 2 in **15a-e** caused a dramatic loss in the anticancer activity. Replacement of NH-phenyl linker in **9a-e** with NH only in **3a-e** resulted in lower anticancer activity. Further analysis of compounds **3a-e** clearly revealed that the groups on the phenyl ring had a notable influence on activity. Compounds **3c-e** with CF_3 group at *m*-position showed comparable

anticancer activity to doxorubicin. While the introduction of two groups at 2 and 6 positions in compounds **3a** and **3b** resulted in a marked decrease in the activity, suggesting that substitution at 2 and 6 positions of the phenyl ring was not tolerated for this region. Replacement of the orthogonal 4-anilinothienopyrimidine head in **9a-e** and **11a-g** with a rigid coplanar tetracyclic head in **6a-c** and **7a, b** decreased the anticancer activity. It was found that urea derivatives **6 a-c** bearing electron withdrawing group on the phenyl ring were more potent than thiourea derivatives **7a,b** with unsubstituted phenyl ring or phenyl carrying electron donating group. Rigidification of urea or thiourea tail to oxazole or thiazole ring in compounds **10a,b** and **12a,b** resulted in much less anticancer activity. According to these findings, we concluded that a flexible diaryl urea scaffold at 4-position of thieno[2,3-d]pyrimdine core with the terminal phenyl ring bearing electron withdrawing group at *p*-position had a positive effect on antitumor activity.

2. 3. Cell cycle analysis and detection of apoptosis

The most active compound **9c** was selected to further study its effects on cell cycle progression and induction of apoptosis in the MCF-7 cell line. Exposure of MCF-7 cells to compound **9c** at its IC_{50} value for 24h and its effect on the normal cell cycle profile and induction of apoptosis were analyzed. Exposure of MCF-7 cells to compound **9c** resulted in an interference with the normal cell cycle distribution of this cell line. Compound **9c** induced a significant increase in the percentage of cells at pre-G1 and G2/M phases by 15.1 and 2.2 folds, respectively (figure 6) compared to control. Accumulation of cells in pre-G1 phase, confirmed by the presence of a sub-G1 peak in the cell cycle profile analysis, may have resulted from degradation or fragmentation of the genetic materials, indicating a possible role of apoptosis in compound **9c**-induced cancer

cell death and cytotoxicity. On the other hand, the accumulation of the cells in G2/M phase may have resulted from G2 arrest.

2. 4. Apoptosis determination by Annexin-V assay

To ensure the ability of compound **9c** to induce apoptosis, a biparametric cytofluorimetric analysis was performed, using Propidium iodide (PI), which stains DNA and enters only dead cells, and fluorescent immunolabeling of the protein annexin-V, which binds to phosphatidylserine (PS) expressed on the surface of the apoptotic cells and fluoresces green, after interacting with the labeled annexin-V [18]. Dual staining of annexin-V with PI permits discrimination between live cells, early apoptotic cells, late apoptotic cells and necrotic cells. As shown in figure 7, after 24 h of treatment with compound **9c** at its IC_{50} concentration (7.10 μM) a decrease in the percentage of the survived cells was observed. Moreover, a significant increase in the percentage of annexin-V positive cells (30 folds more than control) occurred, indicating an early apoptosis (lower right quadrant).

2. 5. Effect of compound 9c on the level of p53/ Bax/ BCL-2:

Tumor cells can acquire resistance to apoptosis by the expression of the anti-apoptotic proteins such as BCL-2 or by the down-regulation or mutation of the pro-apoptotic proteins, such as Bax. The expression of both BCL-2 and Bax is regulated by the p53 tumor suppressor gene [19]. As compound **9c** showed significant apoptosis inducing ability, further investigation was carried out to measure the apoptotic activity, especially the intrinsic pathway through the evaluation of p53, Bax, BCL-2 and caspase-3. Exposure of MCF-7 cells to compound **9c** at IC_{50} for 24h resulted in significant increase in the expression of the tumor suppressor gene p53 and the pro-apoptotic protein Bax, with consequent reduction of the expression levels of the anti-apoptotic protein BCL-2 compared to the control (Table 4 and figure 8). As a result, the test compound **9c** showed

significant elevation in Bax/ BCL-2 ratio, which supports its ability to promote the therapeutic response in MCF-7 cells.

2. 6. Effect of compound 9c on the level of active caspase-3 (key executer of apoptosis):

Two principle apoptotic pathways were identified, the death receptor (or extrinsic) and the mitochondrial (or intrinsic) pathways [20]. The two pathways converge on the same terminal, which was initiated by the activation of caspase-3 and results in DNA fragmentation [21]. In the current study, compound **9c** significantly elevated the Bax / BCL-2 ratio. Therefore, the subsequent step was to assess the level of active caspase-3, which is the key executer of apoptosis. Treatment of MCF-7 cells with compound **9c** at concentration 7.10 µM produced a significant increase in the level of active caspase-3 (Table 5 and figure 9). In conclusion, compound **9c** showed potent pro-apoptotic effect by induction of the intrinsic mitochondrial pathway of apoptosis.

2. 7. *In vitro* topoisomerase II assay:

As a result of the effect of compound **9c** on S phase of the cell cycle in which DNA replicated and the cell cycle arrested at G2/M phase, the inhibition of topoisomerase II enzyme was suspected as expected mechanism of action of this compound. So, the assay was performed to evaluate the topoisomerase II inhibitory activity. Compound **9c** showed promising activity (IC_{50}= 9.29 µM), which was less than 10 µM and comparable to that of doxorubicin, a known potent topoisomerase II inhibitor (IC_{50} = 3.50 µM), so it proved that compound **9c** exerted its anti-proliferative activity through inhibition of topoisomerase II.

2. 8. Molecular docking of compound 9c in the active site of topoisomerase II

Compound **9c** showed promising activity in the topoisomerase II inhibition assay with IC_{50} value 9.29 µM. At this stage, molecular docking study was carried out to investigate its plausible binding pattern and its interaction with the key amino acids in the active site of the topoisomerase II. The ability of the synthesized compound **9c** to interact with the key amino acids in the active site rationalized its good activity. We used The X-ray crystallographic structure of Topoisomerase II co-crystallized with DNA (PDB ID: 1ZXM). As can be seen in figure 10, compound **9c** interacted by its NH of diaryl urea moiety as an H-bond donor with Thr 744. As H-bond acceptor, it interacted with its C=O group of urea scaffold with Tyr 734. Its docking energy score was -10.92 kcal/mol.

2. 9. *In vitro* VEGFR-2 assay

In order to prove the success of fragment based drug design approach, we extended the biological enzyme assay inhibitory activity to VEGFR-2. The IC_{50} value of compound **9c** was evaluated compared to reference VEGFR-2 inhibitor (sorafenib). Compound **9c** showed excellent VEGFR-2 inhibitory activity, at the sub-micromolar level with IC_{50} value 0.2 µM, which was 2.1 folds more potent than sorafenib (IC_{50} = 0.42 µM).

2. 10. Molecular docking of compound 9c in the active site of VEGFR-2

Docking study was performed for compound **9c**, which showed excellent activity in the VEGFR-2 enzyme inhibition assay, which was 2.1 folds more potent than sorafenib, in order to reveal the binding mode of this compound in the active site of the VEGFR-2. To that end, we used (PDB ID: 4ASD), which has VEGFR-2 co-crystallized with sorafenib as inhibitor. The ability of the synthesized compound **9c** to interact with the same key amino acids in the active site rationalized its excellent activity,

as indicated by its docking pattern and docking score, compared to that of sorafenib (figure 11). As can be seen, compound **9c** interacted by its NH of diayl urea moiety as H-bond donor with the key amino acid Glu 885. As H-bond acceptor, it interacted with its C=O group of urea scaffold with the key amino acid Asp 1046. The N1 of pyrimidine ring interacted as an H-bond acceptor with the Cys 919. Moreover, the superior activity of compound **9c** against VEGFR-2 (IC_{50} = 0.2 µM) was supported by its marked docking score (-16.83 kcal/mol.), which was higher than that of sorafenib (-13.39 kcal/mol).

2. 11. QSAR study

The QSAR study was performed using Discovery Studio 2.5 software (Accelrys Inc., San Diego, CA, USA). A set of 21 compounds (**3a-d**, **6a-c**, **7a,b**, **9a,b**, **9d,e** , **11a-g** and **12a**) was used as a training set for a QSAR modeling. Compounds **9c**, **10a** and **12b** were adopted as an external test subset for validating the QSAR models.

2. 11. 1. QSAR modeling

Many molecular descriptors were calculated for each compound employing a calculated molecular properties module. The 3D structures of the training set analogs were imported into the Discovery Studio to calculate various molecular descriptors for each antitumor active agent. Moreover, energies of highest occupied and lowest unoccupied molecular orbitals (HOMO and LUMO) [22, 23] of each of the training set compounds were determined using this software and imported as additional descriptors. Firstly, Genetic function approximation (GFA) was employed to search for the best possible QSAR regression equation, then Multiple linear regression (MLR) analysis was employed to optimize QSAR models that combine high quality binding pharmacophores with other molecular descriptors and being capable of correlating bioactivity variation across the used training set collection [22, 23]. Equation 1

shows our best performing QSAR models. Figure 12 exhibits the corresponding scatter plots of experimental versus estimated bioactivity values for the training set compounds against MCF-7 breast human tumor cell line. Potency (IC_{50}) (the concentration required to produce 50% inhibition of cell growth compared to the control experiment) against MCF-7 tumor cell line (N = 21, r^2 = 0.814, r^2_{adjusted} = 0.752, $r^2_{\text{prediction}}$ = 0.716).

Equation 1

IC_{50} = 32468 – 1010 Jurs-RPCS – 18675 Rad of Gyration + 286.31 PMI-mag + 156.36 PMI-X − 383.46 PMI-Z.

Abbreviations used: Jurs-RPCS, is the Relative Positive Charge Surface area. Jurs descriptors combines shape and electronic information to characterize molecules; Rad of Gyration, is the radius of gyration, it is a molecular property, defined as the mass weighted. Mathematically, it is the root mean square average distance of all atoms in the molecular system from their centre of mass; PMI-mag, Principal Moment of Inertia, calculates the principal moments of inertia about the principal axes of a molecule; PMI-X, Principal moment of inertia at X axis; PMI-Z, Principal moment of inertia at Z axis. The goodness of the model was validated by squared correlation coefficient (R^2) and residuals between the predicted and experimental activity of the test set and training set (Table 6). R^2 values for MCF-7 cell line QSAR models are 0.814.

2. 11. 2. Validation of QSAR

QSAR models were validated employing leave one-out cross-validation, r^2 (squared correlation coefficient value) and r^2 prediction (predictive squared

correlation coefficient value) [23]. In addition to external validation of the determined QSAR equations was performed utilizing three of our synthesized analogues exhibiting promising (**9c**), mild (**10a**) and inactive

(**12b**) anticancer properties. The observed activities and those provides by QSAR study, are presented in Table 7.

3. Conclusion

In summary, a series of novel tetrahydrobenzothieno[2,3-d]pyrimidine urea derivatives was synthesized according to fragment-based design. They were evaluated for their anticancer activity against MCF-7 cell line. Three compounds **9c**, **9d** and **11b** showed 1.5-1.03 folds more potent anticancer activity than doxorubicin. The most potent compound **9c** showed promising inhibitory activity against topoisomerase II (IC_{50}= 9.29 µM). At the same time, it showed excellent VEGFR-2 inhibitory activity at the sub-micromolar level with IC_{50} value 0.2 µM, which was 2.1 folds more potent than sorafenib. Moreover, it induced a significant increase in the percentage of cells at pre-G1 and G2/M phases by 15.1 and 2.2 folds respectively, compared to control, indicating a possible role of apoptosis in compound **9c**-induced cancer cell death and cytotoxicity. Compound **9c** showed potent pro-apoptotic effect through induction of the intrinsic mitochondrial pathway of apoptosis. This mechanistic pathway was confirmed by a significant increase in the expression of the tumor suppressor gene p53, elevation in Bax/ BCL-2 ratio and a significant increase in the level of active caspase-3, compared to the control. Compound **9c** is a promising multi-targeted lead for the design and synthesis of potent anticancer agents. QSAR studies delivered equations of five 3D descriptors with R^2 = 0.814.The most important and controlling descriptors in anticancer properties were 3D descriptors including Jurs-RPCS, Rad of Gyration, PMI-mag, PMI-X and PMI-Z. External validation of the established QSAR models utilizing three of our synthesized analogues exhibiting promising (**9c**), mild (**10a**) and inactive (**12b**) anticancer properties, revealed good agreement between the experimental and the calculated data. It can be concluded that this QSAR

model provides an effective technique for understanding the observed anticancer properties and thus could be adopted for developing effective lead structures.

4. Experimental

4. 1. Chemistry

4. 1. 1. General

Melting points were obtained on a Griffin apparatus and were uncorrected. Microanalyses for C, H and N were carried out at the Regional Center for Mycology and Biotechnology, Faculty of Pharmacy, Al-Azhar University. IR spectra were recorded on Shimadzu IR 435 spectrophotometer (Shimadzu Corp., Kyoto, Japan) Faculty of Pharmacy, Cairo University, Cairo, Egypt and values were represented in cm^{-1}. ^{1}H NMR spectra were carried out on Bruker 400MHz (Bruker Corp., Billerica, MA, USA) spectrophotometer, Faculty of Pharmacy, Cairo University, Cairo, Egypt. Tetramethylsilane (TMS) was used as an internal standard and chemical shifts were recorded in ppm on δ scale and coupling constants (J) were given in Hz. ^{13}C NMR spectra were carried out on Bruker 100MHz spectrophotometer, Faculty of Pharmacy, Cairo University, Cairo, Egypt. Mass spectra were recorded on a GCMP-QP1000 EX Mass spectrometer. Progress of the reactions were monitored by TLC using precoated aluminum sheet silica gel MERCK 60F 254 and was visualized by UV lamp.

4. 1. 2. General procedure for the preparation of N-aryl-2-(5,6,7,8-tetrahydrobenzo[4,5]thieno[2,3-d]pyrimidin-4-yl)hydrazine carboxamide (3a-e)

A solution of 4-hydrazinyl-5,6,7,8-tetrahydrobenzo[4,5]thieno[2,3-d]pyrimidine (**2**) (0.22 g, 0.001 mol) in methylene chloride (4 mL) at 0 ^{0}C was treated with the selected isocyanate (0.0011 mol) and stirred

overnight as the temperature slowly rose to room temperature. To the resulting suspension, hexane was added to yield more precipitate. The solid was filtered, dried and recrystallized from the suitable solvent to give ***3a-e.***

4. 1. 2.1. N-(2,6-Dichlorophenyl)-2-(5,6,7,8-tetrahydrobenzo[4,5]thieno-[2,3-d]pyrimidin-4-yl)hydrazinecarboxamide **(3a)**. mp 184-186 ^{o}C (toluene); yield 86%; IR (KBr) ν_{max}: 3360, 3236, 3217 (3NH), 1670 (C=O) cm^{-1}; ^{1}H NMR (DMSO-d_6): δ 1.80-1.85 (m, 4H, 2CH_2), 2.75-2.85 (m, 2H, CH_2), 3.05-3.10 (m, 2H, CH_2), 7.25-7.30 (m, 2H, ArH), 7.48 (t, 1H, *J* = 7.24 Hz, ArH), 8.33 (s, 1H, NH, D_2O exchangeable), 8.41 (s, 1H, C2-H), 8.55 (s, 1H, NH, D_2O exchangeable) and 8.62 (s, 1H, NH, D_2O exchangeable) ppm; MS [m/z, %]: 409 [M+2$\dot{1}^{\cdot+}$, 0.52], 4.8 [M+1$\dot{1}^{\cdot+}$, 0.64] and 407 [M$^{\cdot+}$, 0.42]. Anal. Calcd for $C_{17}H_{15}Cl_2N_5OS$ (408.30): C, 50.01; H, 3.70; N, 17.15. Found: C, 50.17; H, 3.68; N, 17.43.

4. 1. 2. 2. N-(2-Chloro-6-methylphenyl)-2-(5,6,7,8-tetrahydrobenzo[4,5]-thieno[2,3-d]pyrimidin-4-yl)hydrazinecarboxamide **(3b)**. mp 178-180 ^{o}C (ethanol); yield 61 % ; IR (KBr) ν_{max}: 3441, 3321, 3271 (3NH), 1662(C=O) cm^{-1}; ^{1}H NMR (DMSO-d_6): δ 1.80-1.85 (m, 4H, 2CH_2), 2.23 (s, 3H, CH_3), 2.80-2.85 (m, 2H, CH_2), 3.00-3.10 (m, 2H, CH_2), 7.12-7.20 (m, 2H, ArH), 7.31 (t, 1H, ArH), 8.17, 8.18 (2s, 1H, NH, D_2O exchangeable), 8.26 (s, 1H, NH, D_2O exchangeable), 8.40 (s, 1H, C2-H), and 8.42, 8.54 (2s, 1H, NH, D_2O exchangeable) ppm; ^{13}C NMR (DMSO-d_6): δ 18.5, 22.2, 22.4, 25.1, 25.3 (5 aliphatic Cs), 112.6, 127.2, 128.2, 129.5, 132.6, 133.5, 134.0, 138.4, 139.3, 142.7, 151.8 157.3 (aromatic Cs) and 166.0 (C=O) ppm. Anal. Calcd for $C_{18}H_{18}ClN_5OS$ (387.89): C, 55.74; H, 4.68; N, 18.06. Found: C, 55.89; H, 4.74; N, 18.31.

4. 1. 2. 3. N-(4-Chloro-3-(trifluoromethyl)phenyl)-2-(5,6,7,8-tetrahydro-benzo[4,5]thieno[2,3-d]pyrimidin-4-yl)hydrazinecarboxamide **(3c)**. mp 188-190 ^{o}C (toluene); yield 73 % ; IR (KBr) ν_{max}: 3309, 3255, 3190 (3NH), 1651 (C=O) cm^{-1}; ^{1}H NMR (DMSO-d$_6$): δ 1.80-1.90 (m, 4H, 2CH$_2$), 2.80-2.90 (m, 2H, CH$_2$), 3.00-3.15 (m, 2H, CH$_2$), 7.69 (d, 1H, *J* = 8.0 Hz, ArH), 7.89 (d, 1H, *J* = 8.0 Hz, ArH), 8.13 (s, 1H, ArH), 8.44 (s, 1H, C2-H), 8.59 (s, 1H, NH, D$_2$O exchangeable), 8.98, 9.40 (2s, 1H, NH, D$_2$O exchangeable), and 10.71 (s, 1H, NH, D$_2$O exchangeable) ppm; MS [m/z, %]: 443 [M+2]$^{\cdot+}$, 0.52] and 441 [M$^{\cdot+}$, 0.90]. Anal. Calcd for $C_{18}H_{15}ClF_3N_5OS$ (441.86): C, 48.93; H, 3.42; N, 15.85. Found: C, 49.08 ; H, 3.45; N, 16.02.

4. 1. 2. 4. N-(2-Fluoro-5-(trifluoromethyl)phenyl)-2-(5,6,7,8-tetrahydro-benzo[4,5]thieno[2,3-d]pyrimidin-4-yl)hydrazinecarboxamide **(3d)**. mp 178-180 ^{o}C (n-hexane); yield 94% ; IR (KBr) ν_{max}: 3421, 3321, 3244 (3NH), 1697 (C=O) cm^{-1}; ^{1}H NMR (DMSO-d$_6$): δ 1.85-1.90 (m, 4H, 2CH$_2$), 2.80-2.90 (m, 2H, CH$_2$), 3.00-3.10 (m, 2H, CH$_2$), 7.41 (s, 1H, ArH), 7.49 (t, 1H, *J* = 10.4 Hz, ArH), 7.61 (t, 1H, *J* = 10.4 Hz, ArH), 8.62 (s, 1H, C2-H), 8.90 (s, 1H, NH, D$_2$O exchangeable), 9.05 (s, 1H, NH, D$_2$O exchangeable) and 9.19, 10.93 (2s, 1H, NH, D$_2$O exchangeable) ppm; ^{13}C NMR (DMSO-d$_6$): δ 22.2, 22.4, 25.2, 25.9 (4 aliphatic Cs), 112.8, 113.5, 115.9, 116.1, 116.5, 116.7 (aromatic Cs), 122.7 (CF$_3$), 125.5, 125.9, 127.0, 128.2, 134.2, 137.2 (aromatic Cs) and 155.9 (C=O) ppm. Anal. Calcd for $C_{18}H_{15}F_4N_5OS$ (425.4): C, 50.82; H, 3.55; N, 16.46. Found: C, 50.93; H, 3.51; N, 16.58.

4. 1. 2. 5. 2-(5,6,7,8-Tetrahydrobenzo[4,5]thieno[2,3-d]pyrimidin-4-yl)-N-(3-(trifluoromethyl)phenyl)hydrazinecarboxamide **(3e)**. mp 168-170 ^{o}C (methylene chloride); yield 89% ; IR (KBr) ν_{max}: 3290, 3267, 3217 (3NH), 1670 (C=O) cm^{-1}; ^{1}H NMR (DMSO-d$_6$): δ 1.80-1.90 (m, 4H,

$2CH_2$), 2.80-2.90 (m, 2H, CH_2), 3.00-3.10 (m, 2H, CH_2), 7.27-7.29 (m, 1H, ArH), 7.47-7.49 (m, 1H, ArH), 7.72-7.74 (m, 1H, ArH), 7.97 (s, 1H, ArH), 8.00 (s, 1H, NH, D_2O exchangeable), 8.32 (s, 1H, NH, D_2O exchangeable), 8.45 (s, 1H, C2-H) and 8.78, 9.46 (2s, 1H, NH, D_2O exchangeable) ppm;. Anal. Calcd for $C_{18}H_{16}F_3N_5OS$ (407.41): C, 53.06; H, 3.96; N, 17.19. Found: C, 53.49; H, 4.01; N, 17.32.

4. 1. 3. Procedure for the preparation of 2-(5,6,7,8-tetrahydrobenzo-[4,5]thieno[2,3-d]pyrimidin-4-yl)hydrazinecarbothioamide (4)

A mixture of 4-chloro-5,6,7,8-tetrahydrobenzo[4,5]thieno[2,3-d]pyrimidine (**1**) (0.23 g, 0.001 mol) and thiosemicarbazide (0.1 g, 0.001 mol) in absolute ethanol (30 mL) was heated under reflux for 8 h. The separated solid was filtered while hot, dried and recrystallized from ethanol to give **4**. mp 212-214 ^oC; yield 71% ; IR (KBr) ν_{max}: 3417, 3302, 3147 (NH_2, 2NH), 1292 (C=S) cm^{-1}; ^1H NMR (DMSO-d_6): δ 1.75-1.85 (m, 4H, $2CH_2$), 2.75-2.80 (m, 2H, CH_2), 3.00-3.05 (m, 2H, CH_2), 7.67, 7.77 (2s, 2H, NH_2, D_2O exchangeable), 8.39 (s, 1H, C2-H), 8.63 (s, 1H, NH, D_2O exchangeable) and 9.29 (s, 1H, NH, D_2O exchangeable) ppm; ^{13}C NMR (DMSO-d_6): δ 22.3, 22.5, 25.3, 25.6 (4 aliphatic Cs), 116.2, 127.0, 133.7, 152.5, 157.1, 165.4 (aromatic Cs) and 182.2 (C=S) ppm. Anal. Calcd for $C_{11}H_{13}N_5S_2$ (279.38): C, 47.29; H, 4.69; N, 25.07. Found: C, 47.54; H, 4.76; N, 25.34.

4. 1. 4. Procedure for the preparation of 8,9,10,11-tetrahydrobenzo-[4,5]thieno[3,2-e][1,2,4]triazolo[4,3-c]pyrimidin-3-amine (5)

A mixture of 4-chloro-5,6,7,8-tetrahydrobenzo[4,5]thieno[2,3-d]pyrimidine (**1**) (0.23 g, 0.001 mol) and thiosemicarbazide (0.1 g, 0.001 mol) in absolute ethanol (30 mL) was heated under reflux for 20 h. The reaction mixture was cooled, then the separated solid was filtered, dried

and recrystallized from ethanol to give **5**. mp 212-214 ^{o}C; yield 77% ; IR (KBr) ν_{max}: 3282, 3221 (NH_2) cm^{-1}; ^{1}H NMR (DMSO-d_6): δ 1.80-1.90 (m, 4H, $2CH_2$), 2.80-2.85 (m, 2H, CH_2), 2.90-2.95 (m, 2H, CH_2), 6.45 (s, 2H, NH_2, D_2O exchangeable) and 9.14 (s, 1H, C2-H) ppm. Anal. Calcd for $C_{11}H_{11}N_5S$ (245.30): C, 53.86; H, 4.52; N, 28.55. Found: C, 54.12; H, 4.60; N, 28.81.

4. 1. 5. General procedure for the preparation of 1-aryl-3-(8,9,10,11-tetrahydrobenzo[4,5]thieno[3,2-e][1,2,4]triazolo[4,3-c]pyrimidin-3-yl)urea (6a-c)

A solution of 8,9,10,11-tetrahydrobenzo[4,5]thieno[3,2-e][1,2,4]-triazolo[4,3-c]pyrimidin-3-amine (**5)** (0.23 g, 0.001 mol) in methylene chloride (4 mL) at 0 □C was treated with the selected isocyanate (0.0011 mol) and stirred overnight as the temperature slowly rose to room temperature. To the resulting suspension, hexane was added to yield more precipitate. The solid was filtered, dried and recrystallized from the suitable solvent to give **6a-c.**

***4. 1. 5. 1.* 1-(2-Chloro-6-methylphenyl)-3-(8,9,10,11-tetrahydrobenzo-[4,5] thieno [3,2-e][1,2,4]triazolo[4,3-c]pyrimidin-3-yl)urea (6a)** mp 162-164 ^{o}C (ethanol); yield 44% ; IR (KBr) ν_{max}: 3255, 3217 (2NH), 1650 (C=O) cm^{-1}; ^{1}H NMR (DMSO-d_6): δ 1.80-1.90 (m, 4H, $2CH_2$), 2.29 (s, 3H, CH_3), 2.80-2.90 (m, 2H, CH_2), 2.95-3.05 (m, 2H, CH_2), 7.05 (s, 1H, NH, D_2O exchangeable), 7.17-7.38 (m, 3H, ArH), 9.16 (s, 1H, C2-H) and 9.89 (s, 1H, NH, D_2O exchangeable) ppm; ^{13}C NMR (DMSO-d_6): δ 18.9, 22.1, 22.9, 25.2, 25.4 (5 aliphatic Cs), 118.0, 127.4, 127.6, 128.4, 129.4, 129.6, 132.4, 135.8, 136.8, 138.9, 139.2, 148.6, 153.3 (aromatic Cs) and 167.1 (C=O) ppm. Anal. Calcd for $C_{19}H_{17}ClN_6OS$ (412.90): C, 55.27; H, 4.15; N, 20.35. Found: C, 55.45; H, 4.23; N, 20.59.

4. 1. 5. 2. **1-(2-Fluoro-5-(trifluoromethyl)phenyl)-3-(8,9,10,11-tetrahydrobenzo[4,5]thieno[3,2-e][1,2,4]triazolo[4,3-c]pyrimidin-3-yl)urea (6b)** mp 138-140 ^{o}C (ethanol); yield 36% ; IR (KBr) ν_{max}: 3379, 3224 (2NH), 1666 (C=O) cm^{-1}; ^{1}H NMR (DMSO-d$_6$): δ 1.75-1.95 (m, 4H, 2CH$_2$), 2.80-2.90 (m, 2H, CH$_2$), 2.95-3.00 (m, 2H, CH$_2$), 7.11 (s, 1H, NH, D$_2$O exchangeable), 7.37-7.53 (m, 2H, ArH), 9.12 (s, 1H, ArH), 9.15 (s, 1H, C2-H) and 9.59 (s, 1H, NH, D$_2$O exchangeable) ppm; ^{13}C NMR (DMSO-d$_6$): δ 22.1, 22.9, 25.2, 25.4 (4 aliphatic Cs), 118.0, 120.2, 122.9 (CF$_3$), 125.6, 128.3, 128.5, 128.6, 135.7, 136.7, 145.2, 148.6, 152.4, 154.2, 164.2 (aromatic Cs) and 167.0 (C=O) ppm. Anal. Calcd for $C_{19}H_{14}F_4N_6OS$ (450.41): C, 50.67; H, 3.13; N, 18.66. Found: C, 50.84; H, 3.16; N, 18.92.

4. 1. 5. 3. **1-(8,9,10,11-Tetrahydrobenzo[4,5]thieno[3,2-e][1,2,4]triazolo [4,3-c]pyrimidin-3-yl)-3-(3-(trifluoromethyl)phenyl)urea (6c)** mp 148-150 ^{o}C (isopropanol); yield 38% ; IR (KBr) ν_{max}: 3255, 3151 (2NH), 1670 (C=O) cm^{-1}; ^{1}H NMR (DMSO-d$_6$): δ 1.85-1.95 (m, 4H, 2CH$_2$), 2.85-2.90 (m, 2H, CH$_2$), 2.95-3.00 (m, 2H, CH$_2$), 7.17 (s, 1H, NH, D$_2$O exchangeable), 7.30 (s, 1H, ArH), 7.43 (s, 1H, C2-H), 7.52-7.56 (m, 1H, ArH), 7.67-7.71 (m, 1H, ArH), 7.95-8.01 (m, 1H, ArH) and 9.15, 9.87 (2s, 1H, NH, D$_2$O exchangeable) ppm; MS [m/z, %]: 432 [M$^{\cdot+}$, 0.91]. Anal. Calcd for $C_{19}H_{15}F_3N_6OS$ (432.42): C, 52.77; H, 3.50; N, 19.43. Found: C, 53.02; H, 3.54; N, 19.60.

4. 1. 6. General procedure for the preparation of 1-aryl-3-(8,9,10,11-tetrahydrobenzo[4,5]thieno[3,2-e][1,2,4]triazolo[4,3-c]pyrimidin-3-yl)thiourea (7a,b)

An equimolar mixture of 8,9,10,11-tetrahydrobenzo[4,5]thieno[3,2-e][1,2,4]triazolo[4,3-c]pyrimidin-3-amine (**5**) (1.23 g, 0.005 mol)**,** the selected isothiocyanate (0.005 mol) and anhydrous potassium carbonate (0.70 g, 0.005 mol) in dioxane (25 mL) was heated under reflux for 25 h. The reaction mixture was cooled, poured into ice cold water (50 mL) and the separated solid was filtered, dried and recrystallized from ethanol to give ***7a,b***.

4. 1. 6. 1. 1-Phenyl-3-(8,9,10,11-tetrahydrobenzo[4,5]thieno[3,2-e]-[1,2,4]triazolo[4,3-c]pyrimidin-3-yl)thiourea **(7a)** mp 108-110 ^{o}C; yield 76% ; IR (KBr) ν_{max}: 3421, 3344 (2NH), 1219 (C=S) cm^{-1}; ^{1}H NMR (DMSO-d_6): δ 1.75-1.90 (m, 4H, 2CH_2), 2.65-2.80 (m, 2H, CH_2), 2.85-3.00 (m, 2H, CH_2), 6.46 (s, 1H, NH, D_2O exchangeable), 7.15-7.65 (m, 5H, ArH), 8.54 (s, 1H, C2-H) and 9.15 (s, 1H, NH, D_2O exchangeable) ppm; ^{13}C NMR (DMSO-d_6): δ 22.7, 22.9, 25.2, 25.4 (4 aliphatic Cs), 118.0, 118.5, 123.8, 128.6, 129.0, 129.3, 132.2, 135.8, 136.8, 148.6, 149.1, 153.4, 167.0 (aromatic Cs) and 174.6 (C=S) ppm. Anal. Calcd for $C_{18}H_{16}N_6S_2$ (380.49): C, 56.82; H, 4.24; N, 22.09. Found: C, 57.06; H, 4.31; N, 22.34.

4. 1. 6. 2. 1-(8,9,10,11-Tetrahydrobenzo[4,5]thieno[3,2-e][1,2,4]triazolo-[4,3-c]pyrimidin-3-yl)-3-(m-tolyl)thiourea (7b) mp 102-104 ^{o}C; yield 42% ; IR (KBr) ν_{max}: 3429, 3313 (2NH), 1249 (C=S) cm^{-1}; ^{1}H NMR (DMSO-d_6): δ 1.80-1.90 (m, 4H, 2CH_2), 2.30 (s, 3H, CH_3), 2.70-2.95 (m, 4H, 2CH_2), 6.45 (s, 1H, NH, D_2O exchangeable), 7.13-7.22 (m, 1H, ArH), 7.25-7.33 (m, 1H, ArH), 7.46 (s, 1H, ArH), 7.55-7.59 (m, 1H, ArH), 9.16 (s, 1H, C2-H) and 10.01, 10.28 (2s, 1H, NH, D_2O exchangeable) ppm. Anal. Calcd for $C_{19}H_{18}N_6S_2$ (394.52): C, 57.84; H, 4.60; N, 21.30. Found: C, 58.11; H, 4.67; N, 21.57.

4. 1. 7. General procedure for the preparation of 1-aryl-3-(4-((5,6,7,8-tetrahydrobenzo[4,5]thieno[2,3-d]pyrimidin-4-yl)amino)phenyl)urea (9a-e)

A solution of N^1-(5,6,7,8-tetrahydrobenzo[4,5]thieno[2,3-d]pyrimidin-4-yl)benzene-1,4-diamine (**8**) (0.90 g, 0.003 mol) in methylene chloride (4 mL) at 0 ^{0}C was treated with the selected isocyanate (0.0033 mol) and stirred overnight as the temperature slowly rose to room temperature. To the resulting suspension, hexane was added to complete precipitation. The solid was filtered, dried and recrystallized from the suitable solvent to give **9a-e**.

4. 1. 7. 1. 1-(2,6-Dichlorophenyl)-3-(4-((5,6,7,8-tetrahydrobenzo[4,5]-thieno[2,3-d]pyrimidin-4-yl)amino)phenyl)urea (9a) mp 258-260 ^{o}C (toluene); yield 55% ; IR (KBr) v_{max}: 3419, 3329, 3309 (3NH), 1635 (C=O) cm^{-1}; ^{1}H NMR (DMSO-d_6): δ 1.75-1.85 (m, 4H, 2CH_2), -2.85 2.75 (m, 2H, CH_2), 3.05-3.10 (m, 2H, CH_2), 6.58 (d, 2H, *J* = 8.2 Hz, ArH), 7.20 (d, 2H, *J* = 8.2 Hz, ArH), 7.44 (d, 2H, *J* = 8.4 Hz, ArH), 7.55 (t, 1H, *J* = 8.4 Hz, ArH), 7.78 (s, 1H, NH, D_2O exchangeable), 8.01 (s, 1H, NH, D_2O exchangeable), 8.11, 8.96 (2s, 1H, NH, D_2O exchangeable) and 8.23 (s, 1H, C2-H) ppm; MS [m/z, %]: 488 [M+5]$^{\cdot+}$, 1.96], 487 [M+4]$^{\cdot+}$, 3.75], 486 [M+3]$^{\cdot+}$, 10.06], 485 [M+2]$^{\cdot+}$, 22.48], 484 [M+1]$^{\cdot+}$, 62.23] and 483 [M$^{\cdot+}$, 27.94]. Anal. Calcd for $C_{23}H_{19}Cl_2N_5OS$ (484.40): C, 57.03; H, 3.95; N, 14.46. Found: C, 57.19; H, 3.98; N, 14.58.

4. 1. 7. 2. 1-(2-Chloro-6-methylphenyl)-3-(4-((5,6,7,8-tetrahydrobenzo-[4,5]thieno[2,3-d]pyrimidin-4-yl)amino)phenyl)urea (9b) mp 268-270 ^{o}C (ethanol); yield 58% ; IR (KBr) v_{max}: 3419, 3365, 3275 (3NH), 1637 (C=O) cm^{-1}; ^{1}H NMR (DMSO-d_6): δ 1.80-1.90 (m, 4H, 2CH_2), 2.26 (s, 3H, CH_3), 2.80-2.90 (m, 2H, CH_2), 3.00-3.15 (m, 2H, CH_2), 7.06-7.22 (m,

3H, ArH), 7.42 (d, 2H, *J* = 8.7 Hz, ArH), 7.52 (d, 2H, *J* = 8.7 Hz, ArH), 7.97 (s, 1H, NH, D_2O exchangeable), 8.10 (s, 1H, NH, D_2O exchangeable), 8.31 (s, 1H, C2-H) and 8.79, 8.91 (2s, 1H, NH, D_2O exchangeable) ppm; ^{13}C NMR (DMSO-d_6): δ 18.9, 22.4, 22.6, 25.5, 25.9 (5 aliphatic Cs), 118.5, 123.8, 127.0, 127.6, 129.1, 129.4, 132.2, 132.9, 133.5, 134.7, 136.4, 139.0, 139.2, 144.7, 152.6, 153.2, 153.6, 155.6 (aromatic Cs) and 165.9 (C=O) ppm. Anal. Calcd for $C_{24}H_{22}ClN_5OS$ (463.98): C, 62.13; H, 4.78; N, 15.09. Found: C, 62.32; H, 4.79; N, 15.18.

4. 1. 7. 3. 1-(4-Chloro-3-(trifluoromethyl)phenyl)-3-(4-((5,6,7,8-tetrahydrobenzo[4,5]thieno[2,3-d]pyrimidin-4-yl)amino)phenyl)urea

(9c) mp 218-220 ^oC (ethanol); yield 74% ; IR (KBr) v_{max}: 3439, 3410, 3321 (3NH), 1635 (C=O) cm^{-1}; ^1H NMR (DMSO-d_6): δ 1.85-1.90 (m, 4H, $2CH_2$), 2.85-2.90 (m, 2H, CH_2), 3.10-3.15 (m, 2H, CH_2), 7.38 (s, 1H, ArH), 7.45 (d, 2H, *J* = 6.0 Hz, ArH), 7.57 (d, 2H, *J* = 6.0 Hz, ArH), 7.61-7.66 (m, 1H, ArH), 8.10-8.14 (m, 1H, ArH), 8.35 (s, 1H, C2-H), 8.90 (s, 1H, NH, D_2O exchangeable), 9.04 (s, 1H, NH, D_2O exchangeable), and 9.35, 9.44 (2s, 1H, NH, D_2O exchangeable) ppm; MS [m/z, %]: 520 [M+3]$^{\cdot+}$, 0.81], 519 [M+2]$^{\cdot+}$, 0.82] and 518 [M+1]$^{\cdot+}$, 1.04]. Anal. Calcd for $C_{24}H_{19}ClF_3N_5OS$ (517.95): C, 55.65; H, 3.70; N, 13.52. Found: C, 55.79 ; H, 3.68; N, 13.69.

4. 1. 7. 4. 1-(2-Fluoro-5-(trifluoromethyl)phenyl)-3-(4-((5,6,7,8-tetrahydrobenzo[4,5]thieno[2,3-d]pyrimidin-4-yl)amino)phenyl)urea

(9d) mp 188-190 ^oC (ethanol); yield 71% ; IR (KBr) v_{max}: 3419, 3383, 3334 (3NH), 1705 (C=O) cm^{-1}; ^1H NMR (DMSO-d_6): δ 1.80 -1.90 (m, 4H, $2CH_2$), 2.80-2.90 (m, 2H, CH_2), 3.10-3.20 (m, 2H, CH_2), 7.39-7.62 (m, 6H, ArH), 8.59 (s, 1H, ArH), 8.61 (s, 1H, C2-H), 9.48 (s, 1H, NH, D_2O exchangeable), 9.50 (s, 1H, NH, D_2O exchangeable) and 9.52 (s, 1H,

NH, D_2O exchangeable) ppm. Anal. Calcd for $C_{24}H_{19}F_4N_5OS$ (501.5): C, 57.48; H, 3.82; N, 13.96. Found: C, 57.63; H, 3.87; N, 14.18.

4. 1. 7. 5. 1-(4-((5,6,7,8-Tetrahydrobenzo[4,5]thieno[2,3-d]pyrimidin-4-yl)amino)phenyl)-3-(3-(trifluoromethyl)phenyl)urea (9e) mp 238-240 ^oC (ethanol); yield 92% ; IR (KBr) ν_{max}: 3419, 3304, 3200 (3NH), 1631 (C=O) cm^{-1}; ^1H NMR (DMSO-d_6): δ 1.80-1.85 (m, 4H, $2CH_2$), -2.85 2.80 (m, 2H, CH_2), 3.10-3.15 (m, 2H, CH_2), 7.30 (d, 2H, *J* = 6.2 Hz, ArH), 7.39-7.61 (m, 3H, ArH), 8.02 (d, 2H, *J* = 6.2 Hz, ArH), 8.11 (s, 1H, ArH), 8.34 (s, 1H, C2-H), 8.88 (s, 1H, NH, D_2O exchangeable), 9.02 (s, 1H, NH, D_2O exchangeable) and 9.24, 9.32 (2s, 1H, NH, D_2O exchangeable) ppm; δ 22.3, 22.4, 25.4, 25.8 (4 aliphatic Cs), 114.5, 116.8, 118.6, 119.9, 122.2, 123.2 (aromatic Cs), 123.8 (CF_3), 125.9, 126.9, 130.4, 133.6, 133.7, 134.2, 135.4, 140.6, 140.7, 152.3, 153.0, 155.4 (aromatic Cs) and 165.4 (C=O) ppm; MS [m/z, %]: 486 [M+3ī$^{\cdot+}$, 1.91], 485 [M+2ī$^{\cdot+}$, 3.92], 484 [M+1ī$^{\cdot+}$, 12.43] and 483 [M$^{\cdot+}$, 5.11]. Anal. Calcd for $C_{24}H_{20}F_3N_5OS$ (483.51): C, 59.62; H, 4.17; N, 14.48. Found: C, 59.84; H, 4.21; N, 14.62.

4. 1. 8. General procedure for the preparation of N^1-(3-aryl-4-(4-bromophenyl)oxazol-2(3H)-ylidene)-N^4-(5,6,7,8-tetrahydrobenzo[4,5]-thieno[2,3-d]pyrimidin-4-yl)benzene-1,4-diamine (10a,b)

A mixture of compound **9b** or **9d** (0.001 mol), 4-bromophenacylbromide (0.001 mol) and anhydrous sodium acetate (0.082 g, 0.001 mol) in absolute ethanol (10 mL) was heated under reflux for 6 h. After cooling, the separated solid was filtered, dried and recrystallized from ethanol to afford **10a,b**.

4. 1. 8. 1. (Z)-N^1-(4-(4-Bromophenyl)-3-(2-chloro-6-methylphenyl)-oxazol-2(3H)-ylidene)-N^4-(5,6,7,8-tetrahydrobenzo[4,5]thieno[2,3-d]-pyrimidin-4-yl)benzene-1,4-diamine (10a) mp 208-210 ^{o}C; yield 83% ; IR (KBr) ν_{max}: 3417 (NH) cm^{-1}; ^{1}H NMR (DMSO-d_6): δ 1.80-1.90 (m, 4H, 2CH_2), 2.27 (s, 3H, CH_3), 2.80-2.85 (m, 2H, CH_2), 3.10-3.15 (m, 2H, CH_2), 7.09 (d, 2H, *J* = 8.4 Hz, ArH), 7.34 (d, 2H, *J* = 8.0 Hz, ArH), 7.44 (d, 2H, *J* = 8.0 Hz, ArH), 7.50-7.61 (m, 2H, ArH), 7.71 (d, 2H, *J* = 8.4 Hz, ArH), 8.03 (s, 1H, NH, D_2O exchangeable), 8.15 (s, 1H, oxazole H), 8.23 (s, 1H, C2-H), and 8.33 (t, 1H, ArH) ppm; ^{13}C NMR (DMSO-d_6): δ 19.0, 22.4, 22.5, 25.5, 25.9 (5 aliphatic Cs), 116.8, 117.0, 118.4, 120.1, 123.9, 124.2, 127.1, 127.2, 127.4, 127.5, 129.4, 130.2, 131.7, 132.1, 132.2, 132.4, 133.0, 133.2, 133.3, 134.5, 136.6, 138.9, 152.5, 153.4, 155.5, 155.6 and 166.0 (aromatic Cs) ppm. Anal. Calcd for $C_{32}H_{25}BrClN_5OS$ (643.00): C, 59.77; H, 3.92; N, 10.89. Found: C, 60.04; H, 3.97; N, 11.18.

4. 1. 8. 2. (Z)-N^1-(4-(4-Bromophenyl)-3-(2-fluoro-5-(trifluoromethyl)-phenyl)oxazol-2(3H)-ylidene)-N^4-(5,6,7,8-tetrahydrobenzo[4,5]thieno-[2,3-d]pyrimidin-4-yl)benzene-1,4-diamine (10b) mp 214-216 ^{o}C; yield 85% ; IR (KBr) ν_{max}: 3417 (NH) cm^{-1}; ^{1}H NMR (DMSO-d_6): δ 1.80-1.90 (m, 4H, 2CH_2), 2.80-2.85 (m, 2H, CH_2), 3.15-3.20 (m, 2H, CH_2), 7.37 (d, 2H, *J* = 8.8 Hz, ArH), 7.47 (d, 2H, *J* = 8.4 Hz, ArH), 7.62 (d, 2H, *J* = 8.4 Hz, ArH), 7.66 (d, 2H, *J* = 8.8 Hz, ArH), 7.81 (t, 2H, ArH), 8.23 (s, 1H, C2-H), 8.45 (s, 1H, oxazole H), 8.46 (s, 1H, ArH), and 9.66 (s, 1H, NH, D_2O exchangeable) ppm; ^{13}C NMR (DMSO-d_6): δ 22.4, 22.6, 25.5, 25.8 (4 aliphatic Cs), 114.1, 116.4, 116.5, 116.7, 116.9, 118.7 (aromatic Cs), 123.8 (CF_3), 125.4, 125.6, 127.1, 128.5, 128.6, 128.7, 130.2, 131.7, 131.9, 132.4, 132.5, 133.0, 133.3, 134.1, 135.5, 152.6 (aromatic Cs),

152.8 (C-F), 155.5 and 156.2 (aromatic Cs) ppm. Anal. Calcd for $C_{32}H_{22}BrF_4N_5OS$ (680.51): C, 56.48; H, 3.26; N, 10.29. Found: C, 56.71; H, 3.31; N, 10.47.

4. 1. 9. General procedure for the preparation of 1-aryl -3-(4-((5,6,7,8-tetrahydrobenzo[4,5]thieno[2,3-d]pyrimidin-4-yl)amino)phenyl)thio-urea (11a-g)

A mixture of N^1-(5,6,7,8-tetrahydrobenzo[4,5]thieno[2,3-d]pyrimidin-4-yl)benzene-1,4-diamine (**8**) (1.50 g, 0.005 mol)**,** the selected isothiocyanate (0.005 mol) and anhydrous potassium carbonate (0.70 g, 0.005 mol) in dioxane (25 mL) was heated under reflux for 12 h. The reaction mixture was cooled, poured into ice cold water (50 mL) and the separated solid was filtered, dried and recrystallized from isopropanol to give **11a-g**.

4. 1. 9. 1. 1-Phenyl-3-(4-((5,6,7,8-tetrahydrobenzo[4,5]thieno[2,3-d]-pyrimidin-4-yl)amino)phenyl)thiourea (11a) mp 178-180 ^oC; yield 91% ; IR (KBr) ν_{max}: 3446, 3342, 3257 (3NH), 1222 (C=S) cm^{-1}; ^1H NMR (DMSO-d_6): δ 1.70-1.85 (m, 4H, $2CH_2$), 2.75-2.80 (m, 2H, CH_2), 3.05-3.15 (m, 2H, CH_2), 6.91-7.75 (m, 9H, ArH), 8.33 (s, 1H, C2-H), 9.40 (s, 1H, NH, D_2O exchangeable), 10.63 (s, 1H, NH, D_2O exchangeable) and 10.74 (s, 1H, NH, D_2O exchangeable) ppm; ^{13}C NMR (DMSO-d_6): δ 22.4, 22.6, 25.5, 25.9 (4 aliphatic Cs), 118.6, 119.5, 122.2, 122.6, 123.1, 123.8, 124.0, 127.1, 129.2, 129.7, 140.2, 152.4, 153.0, 160.0 (aromatic Cs) and 172.4 (C=S) ppm; MS [m/z, %]:433 [M+2]$^{\cdot+}$, 0.41] and 432 [M+1]$^{\cdot+}$, 0.56]. Anal. Calcd for $C_{23}H_{21}N_5S_2$ (431.58): C, 64.01; H, 4.90; N, 16.23. Found: C, 64.18; H, 4.96; N, 16.41.

4. 1. 9. 2. 1-(4-Bromophenyl)-3-(4-((5,6,7,8-tetrahydrobenzo[4,5]thieno-[2,3-d]pyrimidin-4-yl)amino)phenyl)thiourea (11b) mp 180-182 ^oC;

yield 58% ; IR (KBr) v_{max}: 3444, 3354, 3334 (3NH), 1222 (C=S) cm^{-1}; ^1H NMR (DMSO-d_6): δ δ 1.80-1.90 (m, 4H, $2CH_2$), 2.80-2.85 (m, 2H, CH_2), 3.10.-3.15 (m, 2H, CH_2), 7.28 (d, 2H, *J* = 7.5 Hz, ArH), 7.55 (d, 2H, *J* = 7.5 Hz, ArH), 7.66 (d, 2H, *J* = 8.4 Hz, ArH), 7.75 (d, 2H, *J* = 8.4 Hz, ArH), 8.36 (s, 1H, C2-H), 9.57 (s, 1H, NH, D_2O exchangeable), 10.60 (s, 1H, NH, D_2O exchangeable) and 10.70 (s, 1H, NH, D_2O exchangeable) ppm; ^{13}C NMR (DMSO-d_6): δ 22.4, 22.6, 25.5, 25.9 (4 aliphatic Cs), 120.6, 121.5, 123.0, 123.8, 124.4, 125.2, 127.0, 127.0, 131.9, 132.1, 132.3, 139.5, 152.4, 155.1 (aromatic Cs) and 172.4 (C=S) ppm; MS [m/z, %]: 512 [M+3]$^{\cdot+}$, 0.25], 511 [M+2]$^{\cdot+}$, 0.20] and 510 [M+1]$^{\cdot+}$, 0.31]. Anal. Calcd for $C_{23}H_{20}BrN_5S_2$ (510.47): C, 54.12; H, 3.95; N, 13.72. Found: C, 54.27; H, 3.98; N, 13.89.

4. 1. 9. 3. 1-(2-Chloro-6-methylphenyl)-3-(4-((5,6,7,8-tetrahydrobenzo-[4,5]thieno[2,3-d]pyrimidin-4-yl)amino)phenyl)thiourea (11c) mp 258-260 ^oC; yield 47% ; IR (KBr) v_{max}: 3448, 3419, 3165 (3NH), 1228 (C=S) cm^{-1}; ^1H NMR (DMSO-d_6): δ 1.80-1.90 (m, 4H, $2CH_2$), 2.37 (s, 3H, CH_3), 2.80-2.85 (m, 2H, CH_2), 3.10.-3.15 (m, 2H, CH_2), 7.32 (d, 2H, ArH), 7.41 (d, 2H, ArH), 7.50-7.74 (m, 3H, ArH), 8.12 (s, 1H, NH, D_2O exchangeable), 8.35 (s, 1H, C2-H), 9.36 (s, 1H, NH, D_2O exchangeable) and 10.03 (s, 1H, NH, D_2O exchangeable) ppm; MS [m/z, %]: 481 [M+2]$^{\cdot+}$, 0.42], 480 [M+1]$^{\cdot+}$, 0.62] and 479 [M$^{\cdot+}$, 0.54]. Anal. Calcd for $C_{24}H_{22}ClN_5S_2$ (510.47): C, 60.05; H, 4.62; N, 14.59. Found: C, 60.23; H, 4.69; N, 14.75.

4. 1. 9. 4. 1-(4-Chlorophenyl)-3-(4-((5,6,7,8-tetrahydrobenzo[4,5]-thieno[2,3-d]pyrimidin-4-yl)amino)phenyl)thiourea (11d) mp 148-150 ^oC; yield 34% ; IR (KBr) v_{max}: 3446, 3412, 3277 (3NH), 1228 (C=S) cm^{-1}; ^1H NMR (DMSO-d_6): δ 1.80-1.90 (m, 4H, $2CH_2$), 2.80-2.85 (m, 2H, CH_2), 3.10.-3.15 (m, 2H, CH_2), 7.33 (d, 2H, ArH), 7.39 (d, 2H, ArH),

7.46 (d, 2H, ArH), 7.58 (d, 2H, ArH), 8.10 (s, 1H, NH, D_2O exchangeable), 8.36 (s, 1H, C2-H), 8.94 (s, 1H, NH, D_2O exchangeable) and 9.95 (s, 1H, NH, D_2O exchangeable) ppm; MS [m/z, %]: 468 [M+3]$^{\cdot+}$, 0.61], 467 [M+2]$^{\cdot+}$, 0.85], 466 [M+1]$^{\cdot+}$, 0.96] and 465 [M$^{\cdot+}$, 0.93]. Anal. Calcd for $C_{23}H_{20}ClN_5S_2$ (466.02): C, 59.28; H, 4.33; N, 15.03. Found: C, 59.41; H, 4.38; N, 15.18.

4. 1. 9. 5. 1-(4-((5,6,7,8-Tetrahydrobenzo[4,5]thieno[2,3-d]pyrimidin-4-yl)amino)phenyl)-3-(m-tolyl)thiourea (11e) mp 168-170 ^{o}C; yield 78% ; IR (KBr) ν_{max}: 3419, 3358, 3205 (3NH), 1228 (C=S) cm^{-1}; ^{1}H NMR (DMSO-d_6): δ 1.80-1.90 (m, 4H, 2CH_2), 2.26 (s, 3H, CH_3), 2.80-2.85 (m, 2H, CH_2), 3.10-3.15 (m, 2H, CH_2), 7.24 (d, 2H, ArH), 7.40 (d, 2H, ArH), 7.59 (s, 1H, ArH), 7.73-7.78 (m, 3H, ArH), 8.24 (s, 1H, NH, D_2O exchangeable), 8.36 (s, 1H, C2-H), 8.95 (s, 1H, NH, D_2O exchangeable) and 10.40 (s, 1H, NH, D_2O exchangeable) ppm; MS [m/z, %]: 447 [M+2]$^{\cdot+}$, 7.67], 446 [M+1]$^{\cdot+}$, 5.83] and 445 [M$^{\cdot+}$, 11.34]. Anal. Calcd for $C_{24}H_{23}N_5S_2$ (445.60): C, 64.69; H, 5.20; N, 15.72. Found: C, 64.63; H, 5.27; N, 15.97.

4. 1. 9. 6. 1-(4-((5,6,7,8-Tetrahydrobenzo[4,5]thieno[2,3-d]pyrimidin-4-yl)amino)phenyl)-3-(p-tolyl)thiourea (11f) mp 174-176 ^{o}C; yield 59% ; IR (KBr) ν_{max}: 3446, 3417, 3354 (3NH), 1226 (C=S) cm^{-1}; ^{1}H NMR (DMSO-d_6): δ 1.80-1.90 (m, 4H, 2CH_2), 2.28 (s, 3H, CH_3), 2.80-2.85 (m, 2H, CH_2), 3.15-3.20 (m, 2H, CH_2), 7.13 (d, 2H, *J* = 8.1 Hz, ArH), 7.35 (d, 2H, *J* = 8.1 Hz, ArH), 7.43 (d, 2H, *J* = 4.8 Hz, ArH), 7.60 (d, 2H, *J* = 4.8 Hz, ArH), 8.11 (s, 1H, NH, D_2O exchangeable), 8.35 (s, 1H, C2-H), 9.57 (s, 1H, NH, D_2O exchangeable) and 9.70 (s, 1H, NH, D_2O exchangeable) ppm; MS [m/z, %]: 447 [M+2]$^{\cdot+}$, 0.39], 446 [M+1]$^{\cdot+}$, 0.59] and 445 [M$^{\cdot+}$, 0.37]. Anal. Calcd for $C_{24}H_{23}N_5S_2$ (445.60): C, 64.69; H, 5.20; N, 15.72. Found: C, 64.88; H, 5.29; N, 15.94.

4. 1. 9. 7. 1-(4-Methoxyphenyl)-3-(4-((5,6,7,8-tetrahydrobenzo[4,5]-thieno[2,3-d]pyrimidin-4-yl)amino)phenyl)thiourea (11g) mp 188-190 ^{o}C; yield 34% ; IR (KBr) ν_{max}: 3446, 3419, 3358 (3NH),1246 (C=S) cm^{-1}; ^{1}H NMR (DMSO-d_6): δ 1.65-1.85 (m, 4H, 2CH_2), 2.80-2.90 (m, 2H, CH_2), 3.10-3.20 (m, 2H, CH_2), 3.70 (s, 3H, OCH_3), 6.98 (d, 2H, ArH), 7.16 (d, 2H, ArH), 7.33 (d, 2H, ArH), 7.50 (d, 2H, ArH), 7.96 (s, 1H, NH, D_2O exchangeable), 8.38 (s, 1H, C2-H), 8.95 (s, 1H, NH, D_2O exchangeable) and 9.95 (s, 1H, NH, D_2O exchangeable) ppm; MS [m/z, %]: 462 [M+1]$^{\cdot+}$, 3.00] and 461 [M$^{\cdot+}$, 5.29]. Anal. Calcd for $C_{24}H_{23}N_5OS_2$ (461.60): C, 62.45; H, 5.02; N, 15.17. Found: C, 62.61; H, 5.11; N, 15.34.

4. 1. 10. General procedure for the preparation of N^1-(3-aryl-4-(4-bromophenyl)thiazol-2(3H)-ylidene)-N^4-(5,6,7,8-tetrahydrobenzo[4,5]-thieno[2,3-d]pyrimidin-4-yl)benzene-1,4-diamine (12a,b)

A mixture of compounds **11a** or **11e** (0.001 mol), 4-bromophenacylbromide (0.001 mol) and anhydrous sodium acetate (0.082 g, 0.001 mol) in absolute ethanol (10 mL) was heated under reflux for 6 h. After cooling, the separated solid was filtered, dried and recrystallized from ethanol to afford ***12a,b***.

4. 1. 10. 1. (Z)-N^1-(4-(4-Bromophenyl)-3-phenylthiazol-2(3H)-ylidene)-N^4-(5,6,7,8-tetrahydrobenzo[4,5]thieno[2,3-d]pyrimidin-4-yl)benzene-1,4-diamine (12a) mp 138-140 ^{o}C; yield 48% ; IR (KBr) ν_{max}: 3387

(NH) cm^{-1}; ^1H NMR (DMSO-d_6): δ 1.80-1.90 (m, 4H, $2CH_2$), 2.80-2.85 (m, 2H, CH_2), 3.10-3.15 (m, 2H, CH_2), 6.75 (s, 1H, NH, D_2O exchangeable) 6.97-7.97 (m, 13H, ArH + 1H of thiazole ring) and 8.52 (s, 1H, C2-H) ppm; ^{13}C NMR (DMSO-d_6): δ 22.6, 24.9, 25.5, 25.9 (4 aliphatic Cs), 118.4, 119.4, 127.1, 128.7, 128.8, 129.0, 129.1, 130.2, 130.5, 131.4, 131.5, 131.7, 132.0, 132.4, 142.0, 143.5, 153.4, 154.9, 156.0, 167.9 and 168.1 (aromatic Cs) ppm; MS [m/z, %]: 614 [M+5]$^{\cdot+}$, 1.38] and 610 [M+1]$^{\cdot+}$, 1.98]. Anal. Calcd for $C_{31}H_{24}BrN_5S_2$ (610.59): C, 60.98; H, 3.96; N, 11.47. Found: C, 61.23; H, 4.02; N, 11.73.

4. 1. 10. 2. (Z)-N^1-(4-(4-Bromophenyl)-3-(m-tolyl)thiazol-2(3H)-ylidene)-N^4-(5,6,7,8-tetrahydrobenzo[4,5]thieno[2,3-d]pyrimidin-4-yl)-benzene-1,4-diamine (12b) mp 148-150 ^oC; yield 79% ; IR (KBr) v_{max}: 3417 (NH) cm^{-1}; ^1H NMR (DMSO-d_6): δ 1.80-1.90 (m, 4H, $2CH_2$), 2.27 (s, 3H, CH_3), 2.80-2.85 (m, 2H, CH_2), 3.10-3.15 (m, 2H, CH_2), 7.05 (d, 2H, ArH), 7.16-7.21 (m, 3H, ArH), 7.38 (d, 2H, ArH), 7.57 (s, 1H, ArH), 7.73 (d, 2H, ArH), 7.84 (d, 2H, ArH), 8.05 (s, 1H, ArH), 8.36 (s, 1H, C2-H) and 8.40 (s, 1H, NH, D_2O exchangeable) ppm; ^{13}C NMR (DMSO-d_6): δ 21.4, 22.4, 22.6, 25.5, 25.8 (5 aliphatic Cs), 121.3, 122.3, 123.1, 124.0, 126.4, 127.0, 129.1, 129.4, 129.9, 130.5, 130.9, 131.6, 132.4, 135.2, 138.1, 138.5, 138.7, 139.2, 152.6, 154.9, 155.5, 165.9 and 166.4 (aromatic Cs) ppm. Anal. Calcd for $C_{32}H_{26}BrN_5S_2$ (624.62): C, 61.53; H, 4.20; N, 11.21. Found: C, 61.71; H, 4.18; N, 11.38.

4. 1. 11. Procedure for the preparation of 2-(((4-aminophenyl)amino)-methyl)-5,6,7,8-tetrahydrobenzo[4,5]thieno[2,3-d]pyrimidin-4(3H)-one (14)

A mixture of 2-(chloromethyl)-5,6,7,8-tetrahydrobenzo[4,5]thieno[2,3-d]pyrimidin-4(3H)-one (**13**) (0.25 g, 0.001 mol), p-phenylene diamine

(0.16 g, 0.0015 mol) and triethylamine (5 drops) in absolute ethanol (18 mL) was heated under reflux for 15 h. The reaction mixture was then cooled, the separated solid was filtered, dried and recrystallized from ethanol to yield **14**. mp 198-200 ^{o}C; yield 78% ; IR (KBr) ν_{max}: 3400, 3329, 3207, 3095 (NH_2, 2NH), 1674 (C=O) cm^{-1}; ^{1}H NMR (DMSO-d_6): δ 1.65-1.85 (m, 4H, $2CH_2$), 2.60-2.85 (m, 4H, $2CH_2$), 4.30 (s, 2H, CH_2NH), 5.75 (s, 2H, NH_2, D_2O exchangeable), 6.61 (d, 2H, *J* = 8.6 Hz, ArH), 7.36 (d, 2H, *J* = 8.6 Hz, ArH), 8.28 (s, 1H, NH, D_2O exchangeable) and 11.55, 12.62 (2s, 1H, NH, D_2O exchangeable) ppm. Anal. Calcd for $C_{17}H_{18}N_4OS$ (326.42): C, 62.55; H, 5.56; N, 17.16. Found: C, 62.80; H, 5.68; N, 17.42.

4. 1. 12. General procedure for the preparation of 1-aryl-3-(4-(((4-oxo-3,4,5,6,7,8-hexahydrobenzo[4,5]thieno[2,3-d]pyrimidin-2-yl)methyl)-amino)phenyl)thiourea (15a-e)

An equimolar mixture of 2-(((4-aminophenyl)amino)methyl)-5,6,7,8-tetrahydrobenzo[4,5]thieno[2,3-d]pyrimidin-4(3H)-one (**14**) (1.63 g, 0.005 mol)**,** the selected isothiocyanate (0.005 mol) and anhydrous potassium carbonate (0.70 g, 0.005 mol) in dioxane (25 mL) was heated under reflux for 25 h. The reaction mixture was cooled, poured into ice cold water (50 mL) and the separated solid was filtered, dried and recrystallized from isopropanol to give **15a-e**.

4. 1. 12. 1. 1-(4-(((4-Oxo-3,4,5,6,7,8-hexahydrobenzo[4,5]thieno[2,3-d]-pyrimidin-2-yl)methyl)amino)phenyl)-3-phenylthiourea (15a) mp 278-280 ^{o}C; yield 60% ; IR (KBr) ν_{max}: 3309, 3271, 3228, 3136 (4NH), 1651 (C=O), 1253 (C=S) cm^{-1}; ^{1}H NMR (DMSO-d_6): δ 1.70-1.85 (m, 4H, $2CH_2$), 2.70-2.80 (m, 2H, CH_2), 2.85-2.95 (m, 2H, CH_2), 3.74 (s, 2H, C***H₂***NH), 7.11-7.19 (m, 3H, ArH), 7.26-7.35 (m, 2H, ArH), 7.45 (d, 2H, *J*

= 7.6 Hz, ArH), 7.49 (d, 2H, *J* = 7.6 Hz, ArH), 8.17 (s, 1H, NH, D_2O exchangeable), 8.70 (s, 1H, NH, D_2O exchangeable), 9.81 (s, 1H, NH, D_2O exchangeable) and 9.83 (s, 1H, NH, D_2O exchangeable) ppm; MS [m/z, %]: 461 [$M^{\cdot+}$, 1.00]. Anal. Calcd for $C_{24}H_{23}N_5OS_2$ (461.60): C, 62.45; H, 5.02; N, 15.17. Found: C, 62.61; H, 5.06; N, 15.29.

4. 1.12.2. 1-(4-Chlorophenyl)-3-(4-(((4-oxo-3,4,5,6,7,8-hexahydrobenzo-[4,5]thieno[2,3-d]pyrimidin-2-yl)methyl)amino)phenyl)thiourea (15b) mp 182-184 ^oC; yield 87% ; IR (KBr) v_{max}: 3309, 3271, 3217, 3136 (4NH), 1651 (C=O), 1253 (C=S) cm^{-1}; ^1H NMR (DMSO-d_6): δ 1.70-1.85 (m, 4H, $2CH_2$), 2.65-2.75 (m, 2H, CH_2), 2.80-2.90 (m, 2H, CH_2), 4.24 (s, 2H, C***H_2***NH), 7.35-7.54 (m, 8H, ArH), 9.86 (s, 1H, NH, D_2O exchangeable), 9.88 (s, 1H, NH, D_2O exchangeable) and 9.96 (s, 2H, 2NH, D_2O exchangeable) ppm. Anal. Calcd for $C_{24}H_{22}ClN_5OS_2$ (496.05): C, 58.11; H, 4.47; N, 14.12. Found: C, 58.37; H, 4.54; N, 14.38.

4. 1. 12. 3. 1-(4-(((4-Oxo-3,4,5,6,7,8-hexahydrobenzo[4,5]thieno[2,3-d]-pyrimidin-2-yl)methyl)amino)phenyl)-3-(m-tolyl)thiourea (15c) mp 158-160 ^oC; yield 52% ; IR (KBr) v_{max}: 3309, 3271, 3217, 3136 (4NH), 1651 (C=O), 1253 (C=S) cm^{-1}; ^1H NMR (DMSO-d_6): δ 1.70-1.85 (m, 4H, $2CH_2$), 2.31 (s, 3H, CH_3), 2.65-2.80 (m, 2H, CH_2), 2.85-2.95 (m, 2H, CH_2), 4.03 (s, 2H, C***H_2***NH), 6.94 (d, 2H, *J* = 8.0 Hz, ArH), 7.19-7.35 (m, 3H, ArH), 7.44 (s, 1H, ArH), 7.62 (d, 2H, *J* = 8.0 Hz, ArH), 9.80 (s, 1H, NH, D_2O exchangeable), 9.84 (s, 1H, NH, D_2O exchangeable), 10.05, 10.10 (2s, 1H, NH, D_2O exchangeable) and 12.14, 12.18 (2s, 1H, NH, D_2O exchangeable) ppm; MS [m/z, %]: 477 [M+2$\dot{1}^{\cdot+}$, 1.57], 476 [M+1$\dot{1}^{\cdot+}$, 2.49] and 475 [$M^{\cdot+}$, 1.73]. Anal. Calcd for $C_{25}H_{25}N_5OS_2$ (475.63): C, 63.13; H, 5.30; N, 14.72. Found: C, 63.38; H, 5.34; N, 14.96.

4. 1. 12. 4. 1-(4-(((4-Oxo-3,4,5,6,7,8-hexahydrobenzo[4,5]thieno[2,3-d]-pyrimidin-2-yl)methyl)amino)phenyl)-3-(p-tolyl)thiourea (15d) mp 188-190 ^{o}C; yield 75% ; IR (KBr) ν_{max}: 3313, 3271, 3217, 3160 (4NH), 1666 (C=O), 1253 (C=S) cm^{-1}; ^{1}H NMR (DMSO-d$_6$): δ 1.70-1.85 (m, 4H, 2CH$_2$), 2.27 (s, 3H, CH$_3$), 2.65-2.90 (m, 4H, 2CH$_2$), 4.03 (s, 2H, C***H$_2$***NH), 7.12 (d, 2H, *J* = 8.0 Hz, ArH), 7.25 (d, 2H, *J* = 8.0 Hz, ArH), 7.35 (d, 2H, *J* = 12.0 Hz, ArH), 7.40 (d, 2H, *J* = 12.0 Hz, ArH), 7.67 (s, 1H, NH, D$_2$O exchangeable), 7.70 (s, 1H, NH, D$_2$O exchangeable), 9.61 (s, 1H, NH, D$_2$O exchangeable) and 9.68 (s, 1H, NH, D$_2$O exchangeable) ppm; ^{13}C NMR (DMSO-d$_6$): δ 20.9, 22.1, 22.9, 25.0, 25.7 (4 Cs of the aliphatic ring + CH$_3$), 52.2 (CH$_2$NH), 118.6, 124.3, 126.2, 127.6, 129.1, 129.3, 130.8, 131.9, 132.1, 134.0, 136.3, 137.3, 138.3 (aromatic Cs), 167.4 (C=O) and 180.0 (C=S) ppm. Anal. Calcd for $C_{25}H_{25}N_5OS_2$ (475.63): C, 63.13; H, 5.30; N, 14.72. Found: C, 63.29; H, 5.37; N, 14.97.

4. 1. 12. 5. 1-(4-Methoxyphenyl)-3-(4-(((4-oxo-3,4,5,6,7,8-hexahydro-benzo[4,5]thieno[2,3-d]pyrimidin-2-yl)methyl)amino)phenyl)thiourea (15e) mp 278-280 ^{o}C; yield 67% ; IR (KBr) ν_{max}: 3309, 3271, 3232, 3200 (4NH), 1654 (C=O), 1246 (C=S) cm^{-1}; ^{1}H NMR (DMSO-d$_6$): δ 1.70-1.85 (m, 4H, 2CH$_2$), 2.70-2.95 (m, 4H, 2CH$_2$), 3.74 (s, 3H, OCH$_3$), 3.78 (s, 2H, C***H$_2$***NH), 6.89 (d, 2H, *J* = 8.8 Hz, ArH), 6.99 (d, 2H, *J* = 8.9 Hz, ArH), 7.31 (d, 2H, *J* = 8.8 Hz, ArH), 7.39 (d, 2H, *J* = 8.9 Hz, ArH), 8.36 (s, 1H, NH, D$_2$O exchangeable), 8.39 (s, 1H, NH, D$_2$O exchangeable) 9.44 (s, 1H, NH, D$_2$O exchangeable) and 9.58, 9.62 (2s, 1H, NH, D$_2$O exchangeable) ppm; ^{13}C NMR (DMSO-d$_6$): δ 22.2, 22.9, 25.6, 25.9 (4 Cs of the aliphatic ring), 55.6 (CH$_2$NH), 56.0 (OCH$_3$), 114.0, 114.4, 115.5, 120.3, 122.6, 124.2, 126.4, 126.7, 127.8, 132.6, 133.3, 154.7, 156.9 (aromatic Cs), 159.0 (C=O) and 180.6 (C=S) ppm.

Anal. Calcd for $C_{25}H_{25}N_5O_2S_2$ (491.63): C, 61.08; H, 5.13; N, 14.25. Found: C, 61.26; H, 5.24; N, 14.42.

4. 2. Biological testing

4. 2. 1. Measurement of potential anti-proliferative activity

The cytotoxic activity of all the newly synthesized compounds was measured *in vitro* on MCF-7 cell line applying Sulforhodamine-B stain (SRB) following the method of Skehan *et al.* [24]. Doxorubicin (Adriamycin ®) was used as a reference standard. Cells were seeded in 96-well microtiter plates at a concentration of $5x10^4$-10^5 cell/well in a fresh medium and left to attach to the plates for 24 h before treatment of the tested compounds. Test compounds were dissolved in dimethylsulfoxide (DMSO) and diluted with saline to the appropriate volume. After 24 h, cells were incubated with the appropriate concentration ranges of drugs (0, 5, 12.5, 25 and 50 µg/mL), the wells were diluted to 200 µL with fresh medium and incubation was continued for 48 h. Control cells were treated with vehicle alone. Four wells were used for each drug concentration. After 48 h incubation, the cells were fixed with 50 µL cold 50 % trichloroacetic acid for 1 h at 4 ^{0}C, washed 5 times with distilled water and then stained for 30 min. at room temperature with 50 µL 0.4 % SRB dissolved in 1% acetic acid. The wells were then washed 4 times with 1% acetic acid. The plates were air-dried and the dye was solubilized with 100 µL/well of 10 mM tris base (PH 10.5) for 5 min. on a shaker (Orbital shaker OS 20, Boeco, Germany) at 1600 rpm.The optical density (O.D.) of each well was measured spectrophotometrically at 564 nm with an enzyme-linked immunosorbent assay (ELISA) microplate reader (Meter tech. Σ 960, U.S.A.). The percentage of cell survival was calculated as follows: Survival fraction = O.D. (treated cells)/ O.D. (control cells). The relation

between surviving fraction and compound concentration was plotted and IC_{50} [the concentration required for 50% inhibition of cell viability] was calculated for each test compound.

4. 2. 2. Cell cycle analysis of compound 9c

The MCF-7 cells were treated with 7.10 µM of compound **9c** for 24 h. After treatment, the cells were washed twice with ice-cold phosphate buffer saline (PBS), collected by centrifugation, and fixed in ice-cold 70% (v/v) ethanol, washed with PBS, re-suspended with 0.1 mg/mL RNase, stained with 40 mg/mL propidium iodide (PI), and analyzed by flow cytometry using FACSCalibur (Becton Dickinson) [25]. The cell cycle distributions were calculated using Cell- Quest software (Becton Dickinson). Exposure of MCF-7 cells to this compound resulted in an interference with the normal cell cycle distribution as indicated.

4. 2. 3. Measurement of apoptosis using Annexin-V-FITC apoptosis

Detection kit

Apoptosis was determined by staining the cells with Annexin V fluorescein isothiocyanate (FITC) and counterstaining with PI using the Annexin V-FITC/PI apoptosis detection kit (BD Biosciences, San Diego, CA) according to the manufacturer's instructions. Briefly, 4×10^6 cell/T 75 flask were exposed to compound **9c** at its IC_{50} concentration (7.10 µM) for 24 h. The cells then were collected by trypsinization and 0.5×10^6 cells were washed twice with phosphate-buffered saline (PBS) and stained with 5 µL Annexin V-FITC and 5 µL PI in 1×binding buffer for 15 minutes at room temperature in the dark. Analyses were performed using FACS Calibur flow cytometer (BD Biosciences, San Jose, CA).

4. 2. 4. Measurement of the effect of compound 9c on the level of p53, Bax, BCL-2 and caspase-3 proteins (Markers of apoptosis):

The levels of the tumor suppressor gene p53, anti-apoptotic marker BCL-2 as well as the apoptotic markers Bax and caspase-3 were assessed using BIORAD iScriptTM One-Step RT-PCR kit with SYBR® Green. The procedure of the used kit was done according to the manufacturer's instructions.

RNA isolation and reverse transcription:

m RNA isolation is carried out using RNeasy extraction kit, up to 1 x 107 cells, depending on the cell line. Cells are disrupted in RNeasy Lysis Buffer (RLT buffer) and homogenized, ethanol is then added to the lysate, creating conditions that promote selective binding of RNA to the RNeasy membrane. The sample is then applied to the RNeasy Mini spin column, total RNA binds to the membrane, contaminants are efficiently was headway, and high quality RNA is eluted in RNase-free water.

Master Mix preparation:

All the following reagents were mixed together to give total volume (50 μL).2X SYBR® Green RT-PCR reaction mixture (25 μL), forward primer (10 μM) (1.5 μL), reverse primer (10 μM) (1.5 μL), nuclease-free H_2O (11 μL), RNA template (1 pg to 100 ng total RNA) (10 μL) and iScript reverse transcriptase for One-Step RT-PCR (1 μL).

Amplification protocol:

Incubate complete reaction mixture in a real-time thermal detection system (Rotorgene) as follows: cDNA synthesis: 10 minutes at 50°C, iScript reverse transcriptase inactivation: 5 minutes at 95°C, polymerase chain reaction (PCR) cycling and detection (30 to 45 cycles): 10 seconds at 95°C and 30 seconds at 55°C to 60°C (data collection step) and melt curve analysis: 1 minute at 95°C and 1 minute at 55°C and 10 seconds at 55°C (80 cycles, increasing each by 0.5°C each cycle).

4. 2. 5. Measurement of inhibitory activity of compound 9c against topoisomerase II

Compound **9c** was selected to be evaluated against topoisomerase II [MBS#942146] using human DNA topoisomerase 2-beta (TOP2B) ELISA kit according to manufacturer's instructions. Prepare all reagents, working standards, and samples. Add 100 µL of standard and sample per well and incubate for 2 h at 37°C. Remove the liquid of each well, don't wash. Add 100 µL of biotin-antibody to each well and incubate for 1 h at 37°C. Aspirate each well and wash three times. Add 100 µL of horseradish peroxidase (HRP-avidin) to each well and incubate for 1 h at 37°C. Repeat the aspiration / wash process for five times. Add 90 µL of 3,3',5,5'-Tetramethylbenzidine (TMB) substrate to each well and incubate for 15-30 minutes at 37°C, protect from light. Add 50 µL of stop solution to each well and determine the optical density of each well within 5 minutes, using a microplate reader set to 450 nm. The values of % activity versus a series of compound concentrations (2.5 µM, 5 µM, 10 µM ,15 µM) were then plotted using non-linear regression analysis of sigmoidal dose-response curve. The IC_{50} values for compound **9c** against topoisomerase II was determined by the concentration causing a half-maximal percent activity and the data were compared with doxorubicin as standard topoisomerase II inhibitor.

4. 2. 6. Measurement of inhibitory activity of compound 9c against VEGFR-2

Compound **9c** was evaluated against VEGFR-2 [RBMS#2019R] using human VEGF-R2/KDR ELISA kit according to manufacturer's instructions. Predilute sample with assay buffer 1:25, determine the number of microwell strips required. Wash microwell strips twice with wash buffer. Add 100 µL assay buffer in duplicate and to all standard wells, pipette 100 µL prepared standard into the first wells and create standard dilutions by transferring 100 µL from well to well. Discard 100 µL from the last wells. Pipette 100 µL of these standard dilutions in the

microwell strips, add 100 µL assay buffer in duplicate to the blank wells and add 50 µL assay buffer to sample wells. Add 50 µL prediluted sample in duplicate to designated sample wells. Prepare biotin-conjugate, add 50 µL biotin-conjugate to all wells and cover microwell strips and incubate 2 h at room temperature (18° to 25°C). Prepare streptavidin-HRP, empty and wash microwell strips 6 times with wash buffer and add 100 µL diluted Streptavidin-HRP to all wells. Cover microwell strips and incubate 1 h at room temperature (18° to 25°C). Empty and wash microwell strips 6 times with wash buffer and add 100 µL of TMB substrate solution to all wells. Incubate the microwell strips for about 30 minutes at room temperature (18° to 25°C). Add 100 µL stop solution to all wells. Blank microwell reader and measure colour intensity at 450 nm. The values of % activity versus a series of compound concentrations (2.5 µM – 5 µM – 10 µM – 15 µM) was then plotted using non-linear regression analysis of sigmoidal dose-response curve. The IC_{50} values for compound **9c** against VEGFR-2 was determined by the concentration causing a half-maximal percent activity and the data were compared with sorafenib as standard VEGFR-2 inhibitor.

4. 2. 7. Molecular Docking of the compound 9c

The molecular modeling of the compound **9c** was carried out using Molecular Operating Environment (MOE, 10.2008) software. All minimizations were performed with MOE until an RMSD gradient of 0.05 kcal $mol^{-1}A°^{-1}$ with MMFF94x force field and the partial charges were automatically calculated. The X-ray crystallographic structure of Topoisomerase II co-crystallized with DNA (PDB ID: 1ZXM) and VEGFR-2 co-crystallized with sorafenib as inhibitor (PDB ID: 4ASD) was downloaded from the protein data bank. The receptor was prepared for docking study using Protonate 3D protocol in MOE with default options followed by water molecules removal. The cocrystalized ligand

was used to define the active site for docking. Triangle Matcher placement method and London dG scoring function were used for docking. Docking setup was first validated by re-docking of the co-crystallized ligand (sorafenib) in the vicinity of the active site of the receptor with energy score (S) = −13.39 kcal/mol. The validated setup was then used in predicting the ligands receptor interactions at the active site for compound **9c**.

Acknowledgments

The authors are grateful to all members of the department of Cancer Biology, National Cancer Institute, Cairo, Egypt, for carrying out the cytotoxicity testing. The authors thank Dr. Esam Rashwan, Head of the confirmatory diagnostic unit VACSERA-EGYPT, for carrying out the cell cycle analysis, apoptosis markers, *in vitro* topoisomerase II and VEGFR-2 inhibition assays. We gratefully acknowledge Prof. Dr. Nasser Ismail, Faculty of Pharmaceutical Sciences and Pharmaceutical Industries, Future University, Cairo, Egypt for carrying out the QSAR studies.

References

[1] Smith, R. A., Cokkinides, V. & Brawley, O. W. Cancer screening in the United States, 2009: a review of current American cancer society guidelines and issues in cancer screening. *CA. Cancer J. Clin.* **59 (1),** 27–41 (2009).

[2] Yadav, B. S., Chanana, P. & Jhamb, S. Biomarkers in triple negative breast cancer: A review. *World J. Clin. Oncol.* **6(6)**, 252-263 (2015).

[3] Pommier, Y., Leo, E., Zhang, H. & Marchand, C. DNA topoisomerases and their poisoning by anticancer and antibacterial drugs. *Chem. Biol.* **17,** 421–433 (2010).

[4] Nitiss, J. L. Targeting DNA topoisomerase II in cancer chemotherapy. *Nat. Rev. Cancer*. **9(5)**, 338-350 (2009).

[5] Bailly, C. Contemporary Challenges in the Design of topoisomerase II inhibitors for cancer chemotherapy. *Chem. Rev.* **112**, 3611-3640 (2012).

[6] Huang, H., Chen, Q., Ku, X., Meng, L., Lin, L., Wang, X., Zhu, C., Wang, Y., Chen, Z., Li, M., Jiang, H., Chen, K., Ding, J. & Liu, H. A series of α-heterocyclic carboxaldehyde thiosemicarbazones inhibit topoisomerase IIα catalytic activity. *J.Med. Chem.* **53(8)**, 3048- 3064 (2010).

[7] Zhao, Y., Wang, C., Wu, Z., Fang, J.&,Zhu, L. Synthesis and antitumor activity of novel aroylthiourea derivatives of podophyllotoxin. Invest. New Drugs. **30 (1)**, 17-24 (2010).

[8] Zhao, Y., Ge, C. W., Wu, Z. H., Wang, C. N., Fang, J. H. & Zhu, L. Synthesis and evaluation of aroylthiourea derivatives of 4-β-amino-4'-O-demethyl-4-desoxypodophyllotoxin as novel topoisomerase II inhibitors. Eur. *J. Med. Chem.* **46(3)**, 901-906 (2011).

[9] Gonzalez, R. E., Lim, C. U., Cole, K., Bianchini, C. H., Schools, G. P., Davis, B. E., Wada, I., Roninson, I. B. & Broude, E. V. Effects of conditional depletion of topoisomerase II on cell cycle progression in mammalian cells. *Cell Cycle* **10 (20)**, 3505-3514 (2011).

[10] Musumeci, F., Radi, M., Brullo, C. & Schenone, S. Vascular endothelial growth factor (VEGF) receptors: drugs and new inhibitors. *J.Med.Chem.* **55 (24),** 10797–10822 (2012).

[11] Richlya, H., Schultheisb, B., Adamietzc, I.A., Kupscha, P., Gruberta, M., Hilgera, R.A., Ludwigd, M., Brendeld, E., Christensene, O.& Strumbergb, D. Combination of sorafenib and doxorubicin in patients with advanced hepatocellular carcinoma: Results from a phase I extension trial. *European Journal of Cancer*. **4 5**, 5 7 9 -5 8 7 (2 0 0 9).

[12] Ullen, A, Farnebo, M., Thyrell, L., Mahmoudi, S., Kharaziha, P., Lennartsson, L., Grander, D., Panaretakis T. & Nilsson, S. Sorafenib induces apoptosis and autophagy in prostate cancer cells *in vitro*. *Int. J. Oncol.* **37**,15–20 (2010).

[13] Liu, Y. & Gray N. S. Rational design of inhibitors that bind to inactive kinase conformations. *Nature Chemical Biology.* **2 (7)**, 358-364 (2006).

[14] Mitchell, T. & Cherry, M. Fragment-based drug design. *Innov. Pharm. Technol.* **16,** 34–36 (2005).

[15] Arya, V. P. Synthesis of new heterocycles: part VI- Synthesis of certain novel condensed thiophenes. *Indian J. Chem.* **10,** 1141–1150 (1972).

[16] Bánhegyi, P., Kéri, G., Örfi, L., Szekélyhidi, Z. & Waczek, F. Tricyclic benzo[4,5]thieno[2,3-d]pyrimidine-4-yl-amines, their salts, process for producing the compounds and their pharmaceutical use. *US Pat. HU 2006000706 A2* (2009).

[17] Shishoo, C. J., Devani, M. B., Bhadti, V. S., Jain, K. S., Rathod, I. S., Goyal, R. K., Gandhi, T. P., Patel, R. B. & Naik, S. R. Synthesis and pharmacological study of antihyperlipaemic activity of 2-substituted thieno[2,3-d]pyrimidin-4(3H)-ones. *Arzneimittelforschung.* **40 (5),** 567–572 (1990).

[18] Vermes, I.; Haanen, C.; Steffens-Nakken, H.; Reutelingsperger, C. J. A novel assay for apoptosis Flow cytometric detection of phosphatidylserine early apoptotic cells using fluorescein labelled expression on Annexin V. *Immunol. Methods* 1995, 184, 39.

[19] Miyashita, T., Krajewski, S., Krajewska, M., Wang, H. G., Lin, H. K., Liebermann, D. A., Hoffman, B. & Reed, J. C. Tumor suppressor p53 is a regulator of bcl-2 and bax gene expression in vitro and in vivo. *Oncogene* **9,** 1799–1805 (1994).

[20] Zimmermann, K. C. & Green, D. R. How cells die: apoptosis pathways. *J. Allergy Clin. Immunol.* **108 (4),** 99–103 (2001).

[21] Elmore, S. Apoptosis: a review of programmed cell death. *Toxicol. Pathol.* **35,** 495–516 (2007).

[22] Girgis, A. S., Stawinski, J., Ismail, N. S.M. & Farag, H . Synthesis and QSAR study of novel cytotoxic spiro[3H-indole-3,2'(1'H)-pyrrolo[3,4-c]pyrrole]-2,3',5'(1H,2'aH,4'H)-triones. *Eur. J. Med. Chem.***47,** 312-322 (2012).

[23] George, R. F., Ismail, N. S.M., Stawinski, J & Girgis A.S. Design, synthesis and QSAR studies of dispiroindole derivatives as new antiproliferative agents. *Eur. J. Med. Chem.***68**, 339-351(2013).

[24] Skehan, P., Storeng, R., Scudiero, D., Monks, A., McMahon, J., Vistica, D., Warren, J. T., Bokesch, H., Kenney, S. & Boyd, M. R. New colorimetric cytotoxicity assay for anticancer-drug screening. *J. Natl. Cancer Inst.* **82 (13),** 1107–1112 (1990).

[25] Tolba, M. F., Esmat, A., Al-Abd, A. M., Azab, S. S., Khalifa, A. E., Mosli, H. A., Abdel-Rahman, S. Z. & Abdel-Naim, A. B. Caffeic acid phenethyl ester synergistically enhances docetaxel and paclitaxel cytotoxicity in prostate cancer cells. *Int. Union Biochem. Mol. Biol.* **65 (8),** 716–729 (2013).

Figure 1: Some structures of the topoisomerase II poisonings or inhibitors, head moieties in blue that represent coplanar polycyclic ring

system that inserts into DNA grooves or ATP domain of topoisomerase enzyme while, tail moieties in red that are composed of acceptor-donner pair hydrogen bond to reinforce interchelating action or enzyme binding affinity.

Figure 2: Examples of diaryl urea derivatives as receptor tyrosine kinase (RTK) inhibitors. Tail substituted phenyl urea moieties are shown in red color that form hydrogen bond with the receptor and head in blue which represent orthogonal polycyclic rings that could act as competitive inhibitor of ATP.

Figure 3: Structural model for rational design of lead template **9a-c** &**11a-g** where head showed in blue and composed of orthogonal 4-anilinotetrahydrobenzothienopyrimidine or large coplanar ring. Tail showed in red and formed from substituted phenyl urea. The structural modification for generation of different models are demonstrated.

Figure 4: Effect of the synthesized molecules **3a-e**, **6a-c**,**7a,b**,**9a-e**,**10a,b**,**11a-g** &**12a,b** at varying concentration (µM) on breast cancer cell line (MCF-7) for 24 h, (A) effect of molecules **3a-e**,(B) effect of molecules **6a-c** &**7a,b**, (C) effect of molecules **9a-e** ,(D) effect of molecules **10a,b** &**12a,b**, (E) effect of molecules **11a-g**,values represent the mean ± SEM for three experiments.

Figure 5: IC_{50} of compounds 3, 6, 7, 9, 10, 11 and 12 in µM against MCF-7 cell line compared to doxorubicin.

Figure 6: Effect of compound **9c** (7.10 µM) on DNA-ploidy flow cytometric analysis of MCF-7 cells after 24 h.

Figure 7: Representative dot plots of MCF-7 cells treated with **9c** (7.10 μM) for 24 h and analyzed by flow cytometry after double staining of the cells with annexin-V FITC and PI.

Figure 8: Graphical representation for p53 / Bax/ BCL-2 analysis of compound **9c** compared to doxorubicin.

Figure 9: Graphical representation for active caspase-3 assay of compound **9c** compared to doxorubicin.

Figure 10: The 2D interaction of **9c** with the DNA binding site of topoisomerase II.

Figure 11: The 2D interaction of ligand (sorafenib) and compound **9c** with the amino acids of the active site of VEGFR-2.

Figure 12: Predicted versus experimental IC_{50} values of the training set compounds against MCF-7 breast human tumor cell line according to Equation 1.

Scheme 1. The synthetic path and reagents for the preparation of the target compounds **2-7**.

Scheme 2. The synthetic path and reagents for the preparation of the target compounds **9-12**.

Scheme 3. The synthetic path and reagents for the preparation of the target compounds **14**, **15**.

Table 1: Results of *in vitro* cytotoxic activity of compounds **3a-e** on MCF-7 cell line.

Table 2: Results of *in vitro* cytotoxic activity of compounds **6 &7** on MCF-7 cell line.

Table 3: Results of *in vitro* cytotoxic activity of compounds **9, 10, 11,** and **12** on MCF-7 cell line.

Table 4: p53 / Bax / BCL-2 analysis results.

Table 5: Active caspase-3 assay results.

Table 6: Estimated activity data of the training set analogs against MCF-7 breast human tumor cell line and calculated descriptors governing activity according to Equation 1.

Table 7: External validation for the established QSAR models utilizing promising (**9c**), mild (**10a**) and inactive (**12b**) anticancer active agents.

Table 1: Results of *in vitro* cytotoxic activity of compounds **3a-e** on MCF-7 cell line:

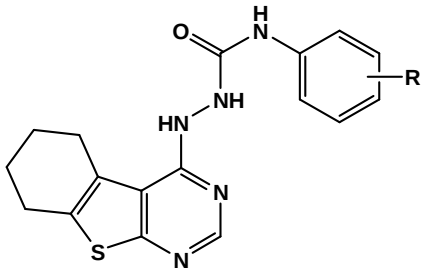

Compound No.	R	IC $_{50}$ (µM*)
3**a**	2,6-$(Cl)_2$	88.90
3**b**	2-Cl,6-CH_3	90.23
3**c**	4-Cl,3-CF_3	53.41
3**d**	2-F,5-CF_3	28.20
3**e**	3-CF_3	22.65
Doxorubicin		10.60

*The values given are means of three experiments.

Table 2: Results of *in vitro* cytotoxic activity of compounds **6 &7** on MCF-7 cell line:

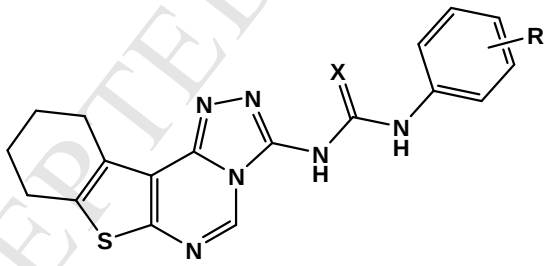

Compound No.	X	R	IC $_{50}$ (µM*)
6a	O	2-Cl,6-CH_3	29.06
6b	O	2-F,5-CF_3	71.93
6c	O	3-CF_3	68.45
7a	S	H	80.90
7b	S	3-CH_3	99.87

*The values given are means of three experiments.

Table 3: Results of *in vitro* cytotoxic activity of compounds **9, 10, 11,** and **12** on MCF-7 cell line:

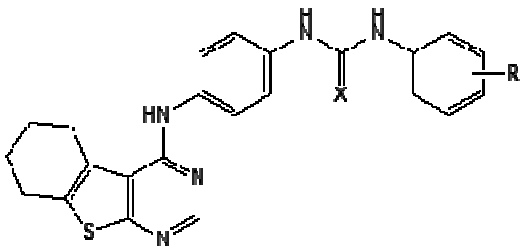

9a-e and **11a-g**

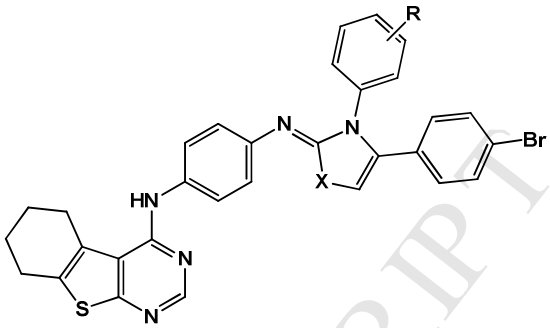

10a,b and **12a,b**

Compound No.	X	R	IC_{50} (µM*)
9a	O	2,6-$(Cl)_2$	103.22
9b	O	2-Cl,6-CH_3	53.88
9c	O	4-Cl,3-CF_3	**7.10**
9d	O	2-F,5-CF_3	**10.33**
9e	O	3-CF_3	51.70
10a	O	2-Cl,6-CH_3	234.80
10b	O	2-F,5-CF_3	-
11a	S	H	48.19
11b	S	4-Br	**9.55**
11c	S	2-Cl,6-CH_3	52.10
11d	S	4-Cl	51.50
11e	S	3-CH_3	38.82
11f	S	4-CH_3	56.10
11g	S	4-OCH_3	79.10
12a	S	H	37.34
12b	S	3-CH_3	-
Doxorubicin			10.60

*The values given are means of three experiments.

Table 4: p53 / Bax / BCL-2 analysis results

	Conc. (IU/mL)		
Compound	**BAX**	**BCL-2**	**p53**
9c	389968	131	77214
Doxorubicin	1824021	8	1271.6
Control	196	538306	244

Table 5: Active caspase-3 assay results

Compound	**Conc. (IU/mL)**
9c	64223
Doxorubicin	363940
Control	75

Table 6: Estimated activity data of the training set analogs against MCF-7 breast human tumor cell line and calculated descriptors governing activity according to Equation 1.

Compd.	Observed activity	Estimated activity	Descriptors				
			Jurs-RPCS	Rad of Gyration	PMI-mag	PMI-X	PMI-Z
3a	88.9	93.3283	0.55018	6.73861	6,830.25	533.205	5,072.08
3b	90.23	106.854	0.58567	6.76998	6,828.3	444.753	5,032.9
3c	53.4	41.704	0.60342	6.76717	6,823.9	445.187	5,030.05
3d	28.2	39.8267	0.60342	6.76705	6,823.84	445.265	5,030.05
6a	29.06	32.2032	0.60342	6.76408	6,816.05	444.404	5,024.05
6b	71.93	71.7469	0.58567	6.76782	6,824.31	445.008	5,030.22
6c	68.45	58.1166	0.58567	6.73826	6,829.83	533.143	5,071.76
7a	80.9	86.4376	0.58567	6.77125	6,828.21	444.924	5,032.9
7b	99.87	75.0248	0.58567	6.76883	6,823.35	444.625	5,029.3
9a	103.22	84.8085	0.60342	6.76857	6,826.52	444.81	5,031.67
9b	53.88	43.5863	0.60342	6.76955	6,828.57	445.616	5,033.59
9d	10.33	7.76832	0.58567	6.77675	6,832.93	445.423	5,036.56
9e	51.7	48.5804	0.60342	6.77449	6,829.35	444.957	5,033.66
11a	48.19	53.9924	0.58567	6.73713	6,828.05	533.732	5,070.74
11b	9.55	17.217	0.60342	6.76454	6,819.87	445.119	5,027.21
11c	52.1	49.3985	0.60342	6.76931	6,823.54	444.846	5,029.52
11d	51.5	54.5301	0.60342	6.77195	6,826.98	444.724	5,031.9
11e	38.82	61.9124	0.60342	6.77079	6,826.82	445.037	5,031.94
11f	56.1	52.7768	0.58567	6.76514	6,818.71	444.756	5,026.12
11g	79.1	72.2958	0.60342	6.76772	6,823.93	444.499	5,029.69
12a	37.34	50.6612	0.60342	6.76775	6,823.62	444.982	5,029.71

Table 7: External validation for the established QSAR models utilizing promising (**9c**), mild (**10a**) and inactive (**12b**) anticancer active agents.

Compd.	Experimental activity	Predicted activity	Jurs-RPCS	Rad of Gyration	PMI-mag	PMI-X	PMI-Z
9c	7.10	9.57	0.57011	6.7717	6,828.02	444.924	5,032.9
10a	234.8	268.58	0.56342	6.77973	6,828.3	444.996	5,032.1
12b	1500	1918.21	0.60342	6.77941	6,829.9	444.989	5,028.9

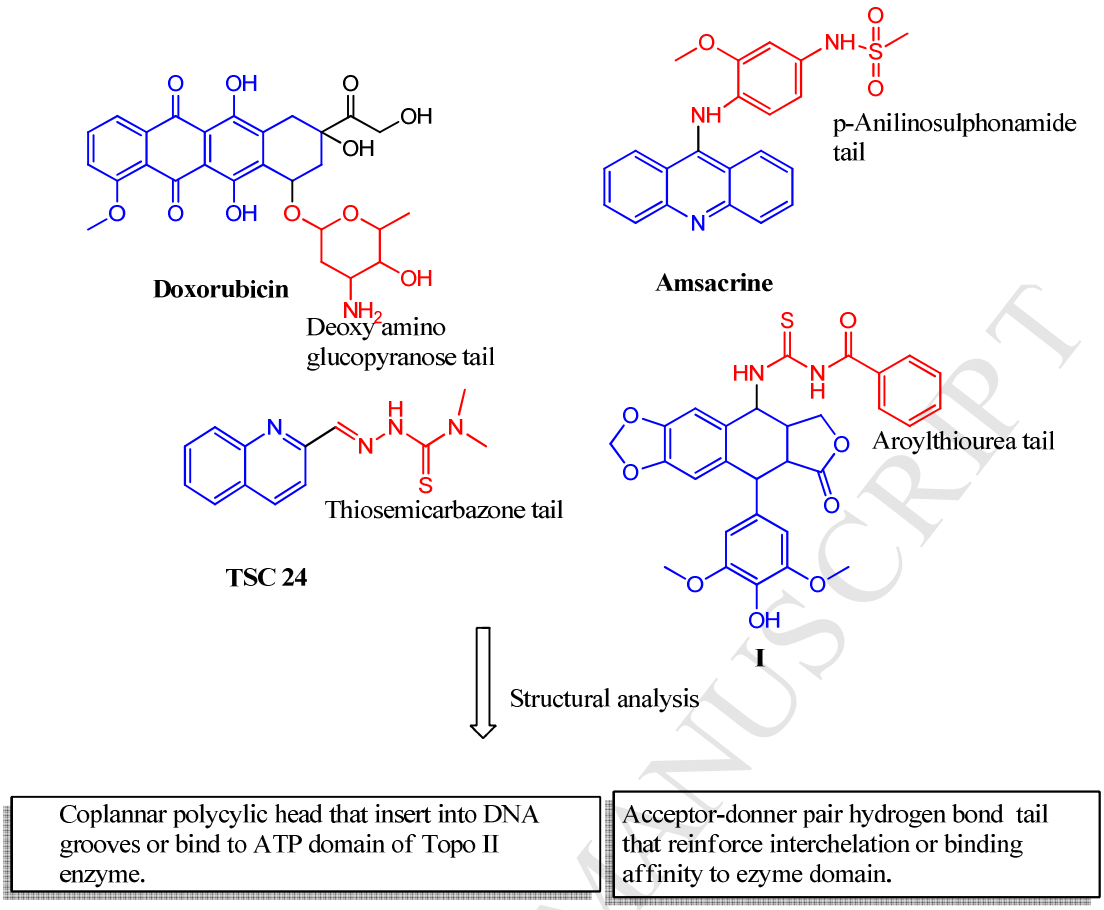

Figure 1: Some structures of the topoisomerase II poisonings or inhibitors, head moieties in blue that represent coplanar polycyclic ring system that inserts into DNA grooves or ATP domain of topoisomerase enzyme while, tail moieties in red that are composed of acceptor-donner pair hydrogen bond to reinforce interchelating action or enzyme binding affinity.

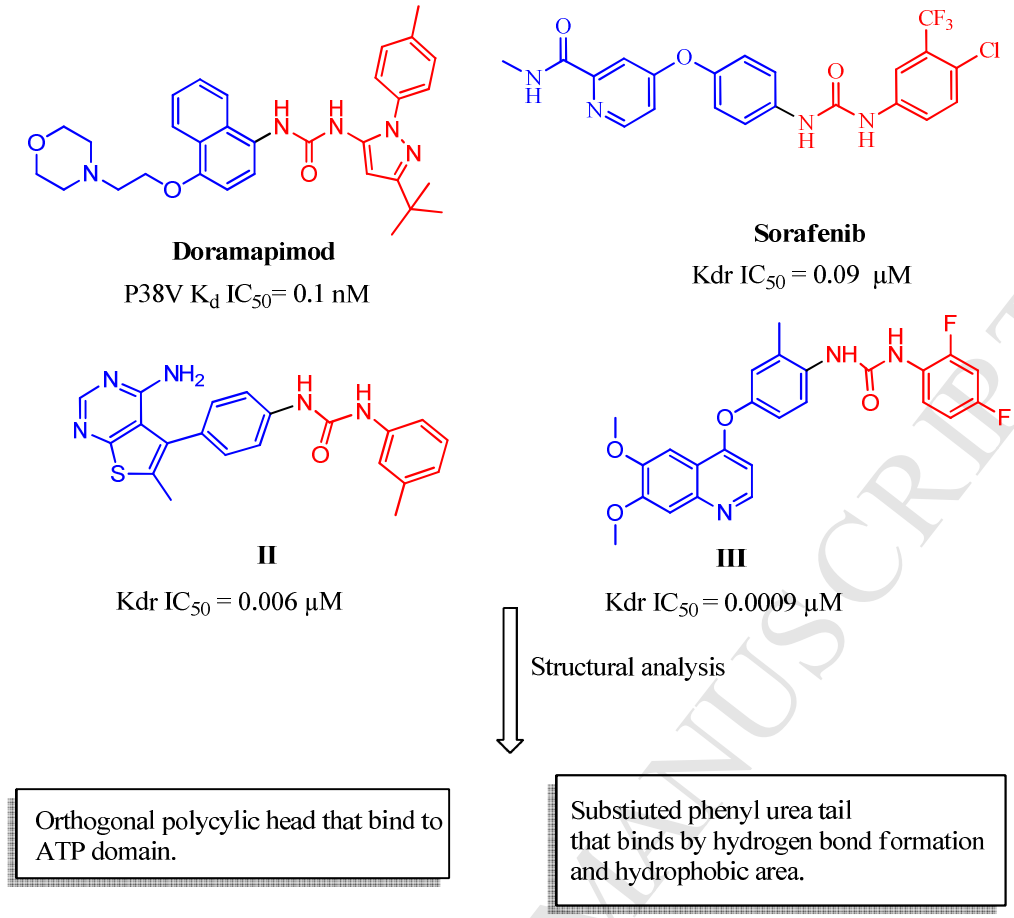

Figure 2: Examples of diaryl urea derivatives as receptor tyrosine kinase (RTK) inhibitors. Tail substituted phenyl urea moieties are shown in red color that form hydrogen bond with the receptor and head in blue which represent orthogonal polycyclic rings that could act as competitive inhibitor of ATP.

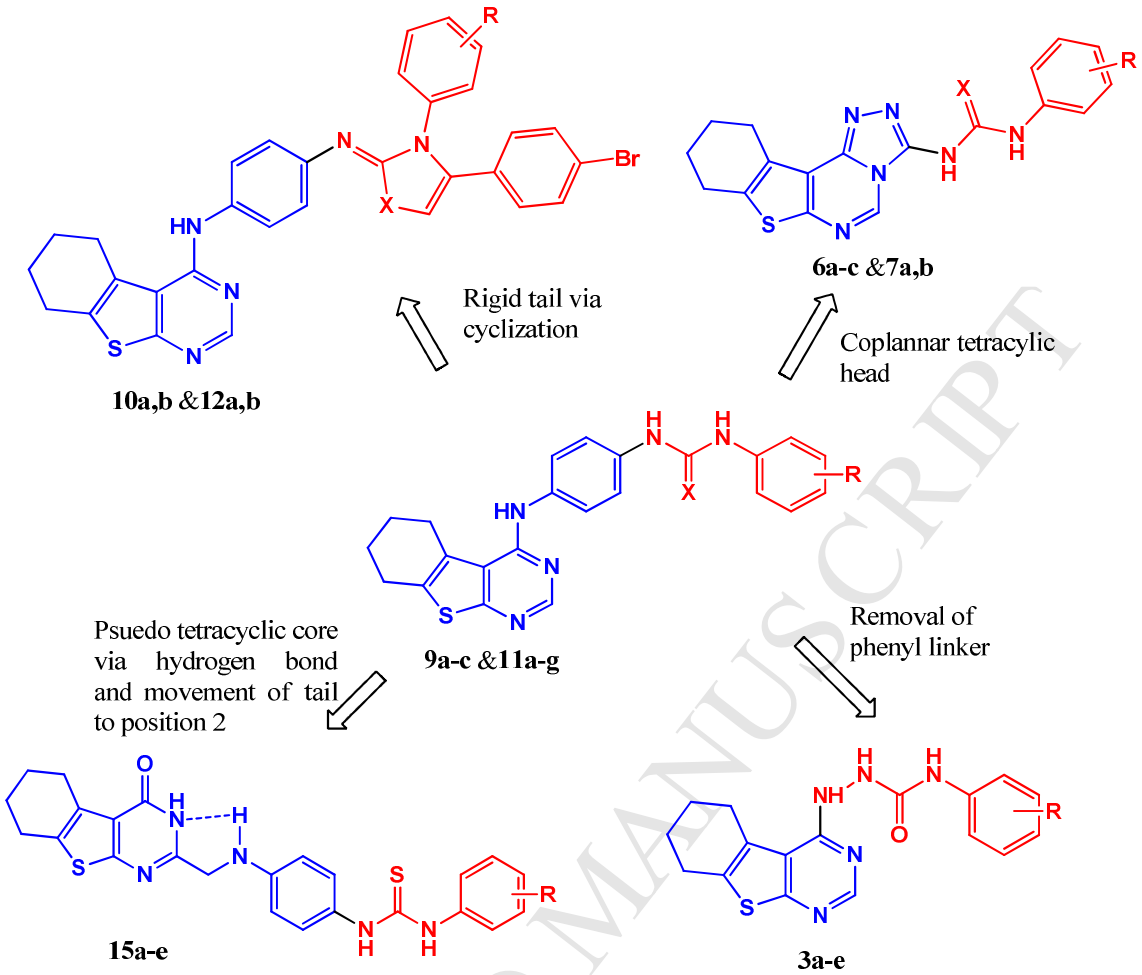

Figure 3: Structural model for rational design of lead template **9a-c &11a-g** where head showed in blue and composed of orthogonal 4-anilinotetrahydrobenzothienopyrimidine or large coplanar ring. Tail showed in red and formed from substituted phenyl urea. The structural modification for generation of different models are demonstrated.

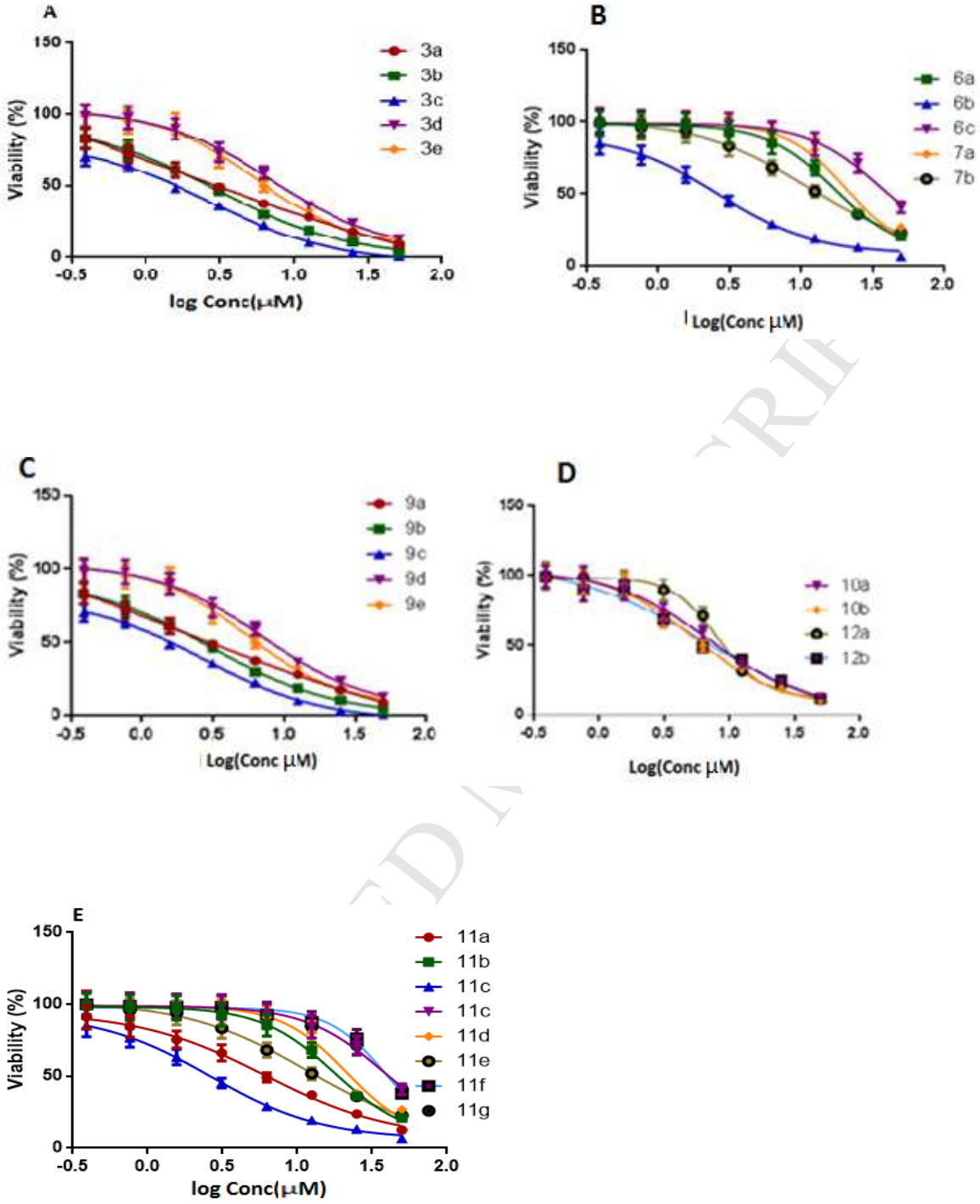

Figure 4: Effect of the synthesized molecules **3a-e**, **6a-c**, **7a,b**, **9a-e**, **10a,b**, **11a-g** & **12a,b** at varying concentrations (µM) on breast cancer cell line (MCF-7) for 24 h, (A) effect of molecules **3a-e**, (B) effect of molecules **6a-c** &**7a,b**, (C) effect of molecules **9a-e** ,(D) effect of molecules **10a,b** &**12a,b**, (E) effect of molecules **11a-g**,values represent the mean ± SEM for three experiments.

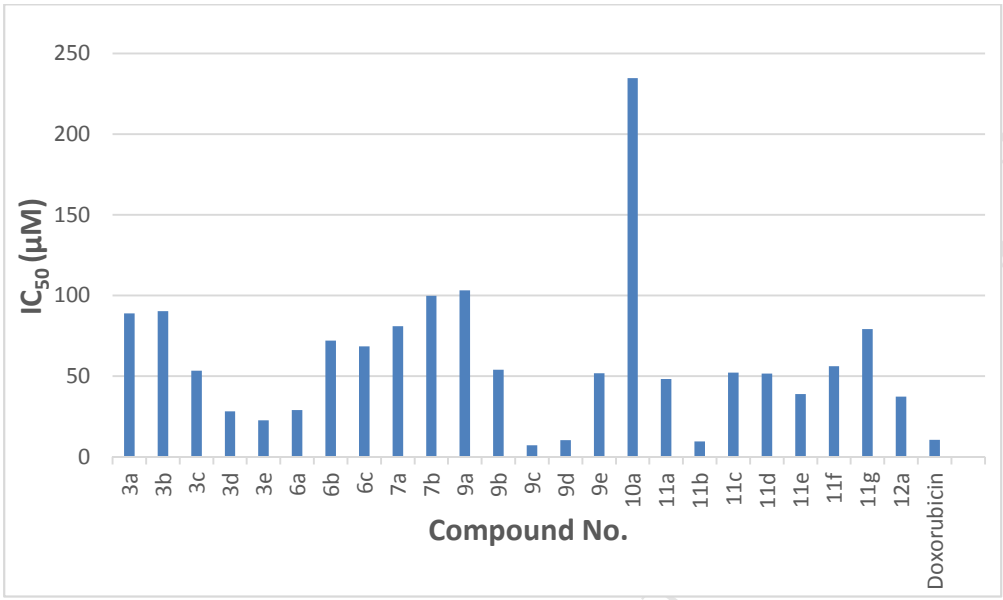

Figure 5: IC_{50} of compounds 3, 6, 7, 9, 10, 11 and 12 in µM against MCF-7 cell line compared to doxorubicin.

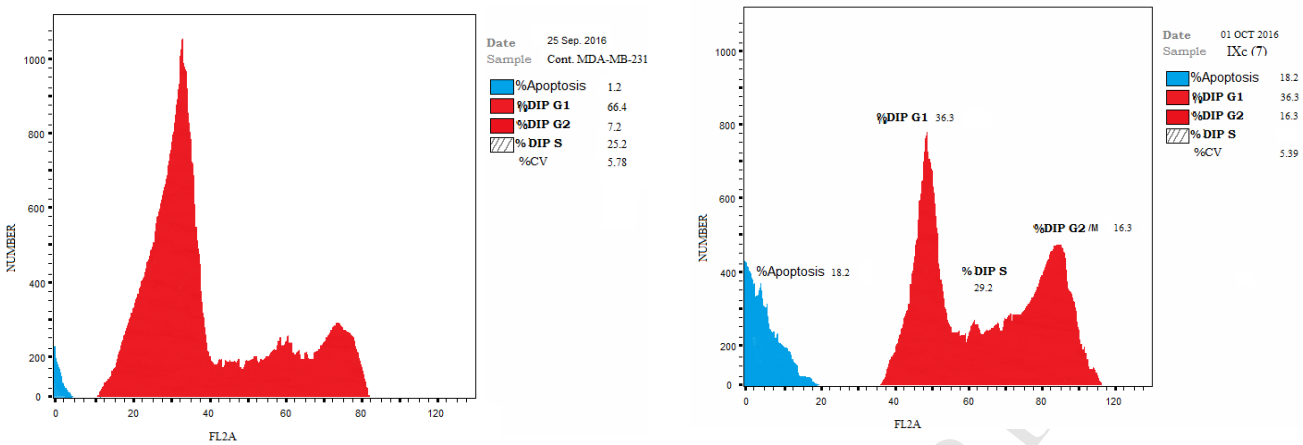

Control **9c**

Figure 6: Effect of compound **9c** (7.10 µM) on DNA-ploidy flow cytometric analysis of MCF-7 cells after 24 h.

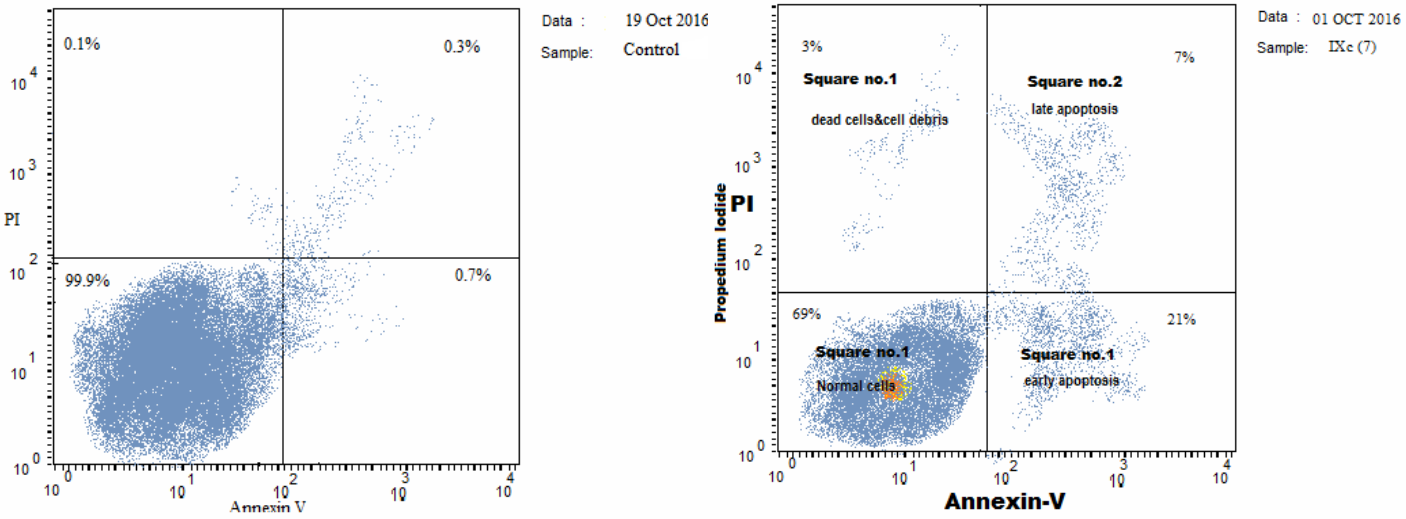

Control 9c

Figure 7: Representative dot plots of MCF-7 cells treated with **9c** (7.10 µM) for 24 h and analyzed by flow cytometry after double staining of the cells with annexin-V FITC and PI.

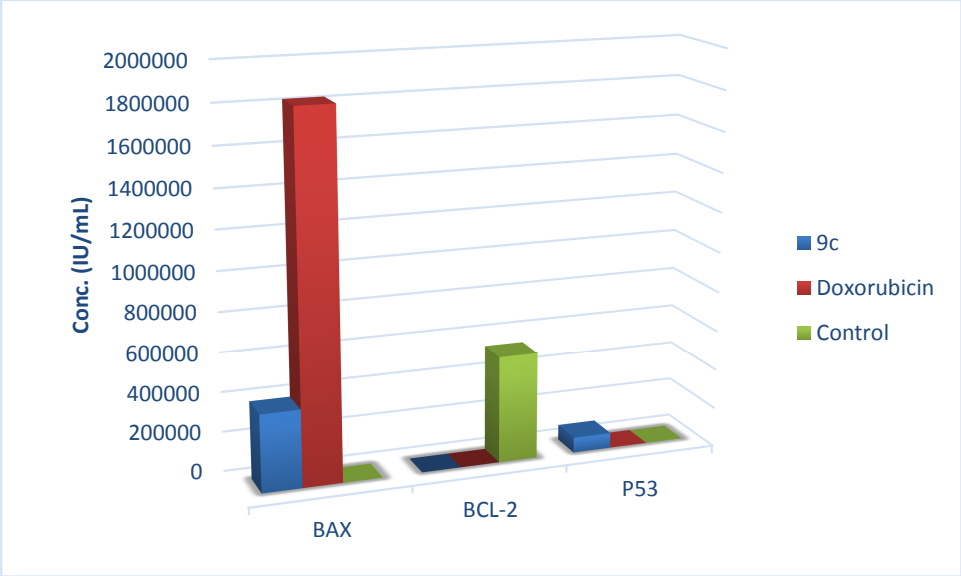

Figure 8: Graphical representation for p53 / Bax/ BCL-2 analysis of compound **9c** compared to doxorubicin.

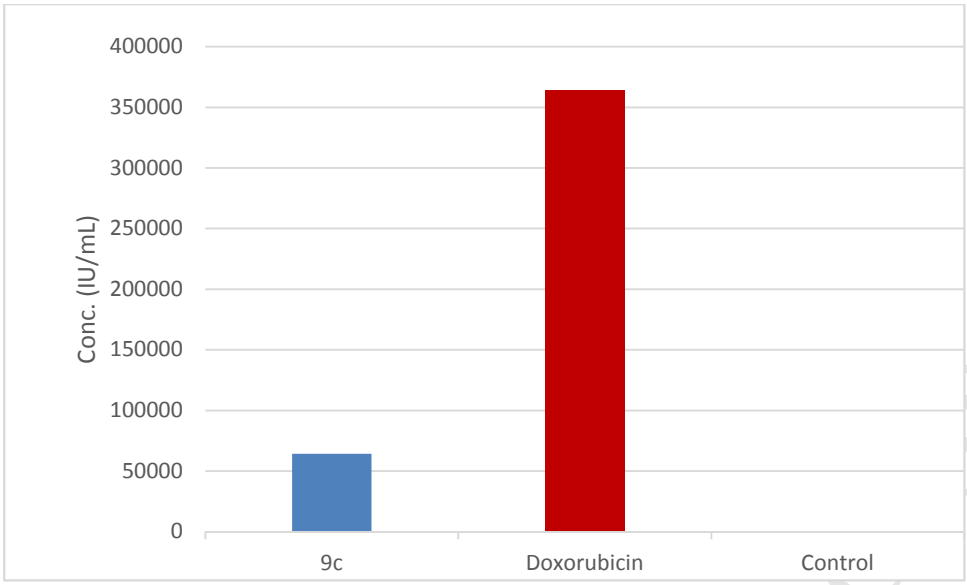

Figure 9: Graphical representation for active caspase-3 assay of compound **9c** compared to doxorubicin.

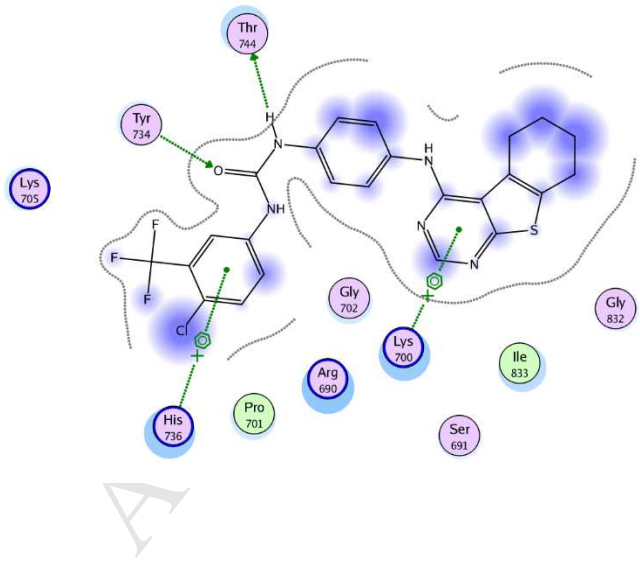

Figure 10: The 2D interaction of **9c** with the DNA binding site of topoisomerase II.

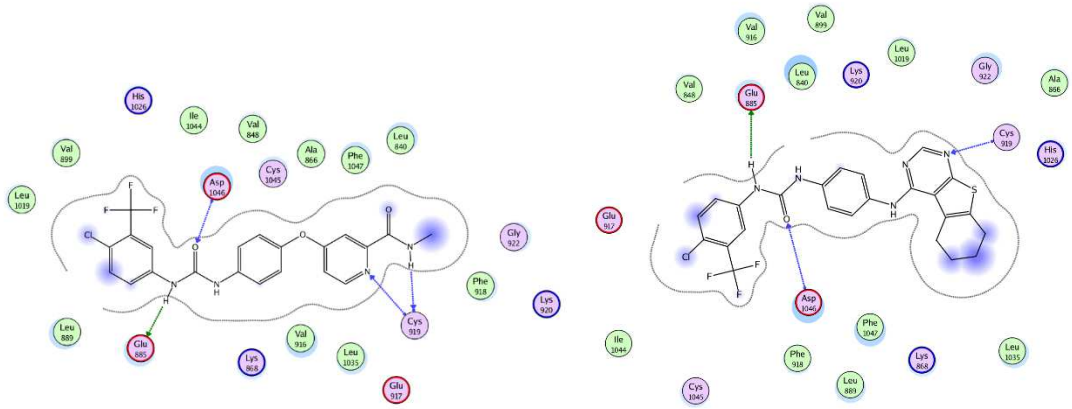

Figure 11: The 2D interaction of ligand (sorafenib) and compound **9c** with the amino acids of the active site of VEGFR-2.

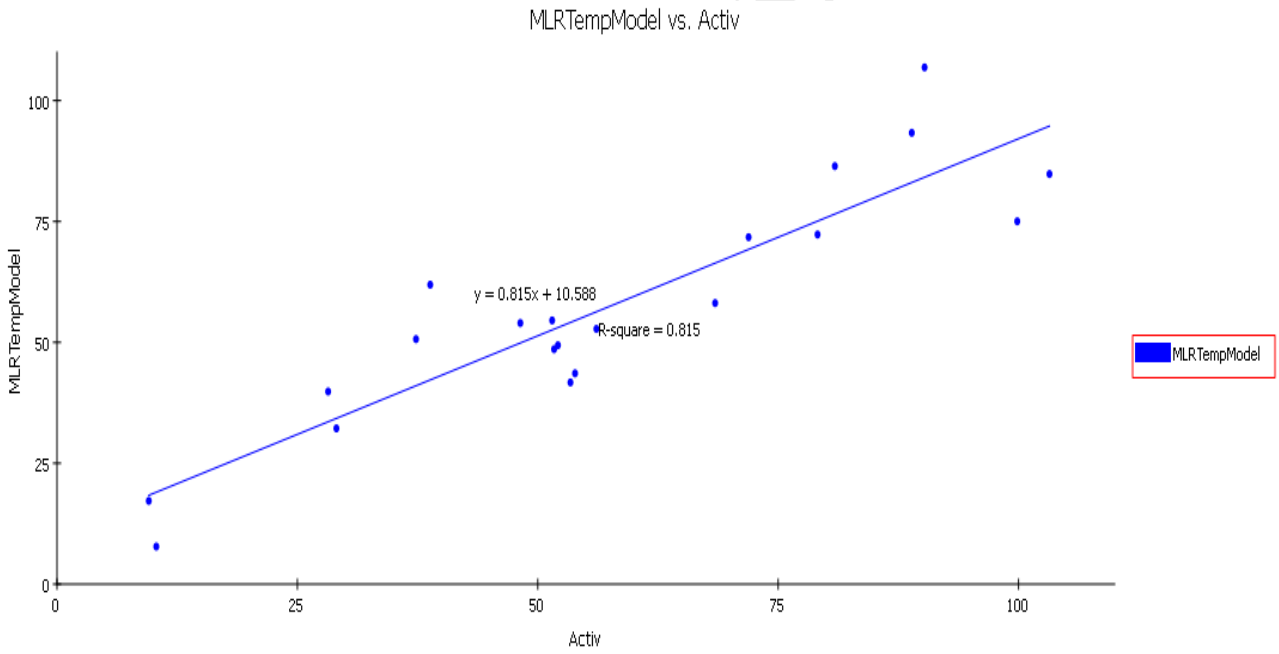

Figure 12: Predicted versus experimental IC_{50} values of the training set compounds against MCF-7 breast human tumor cell line according to Equation 1.

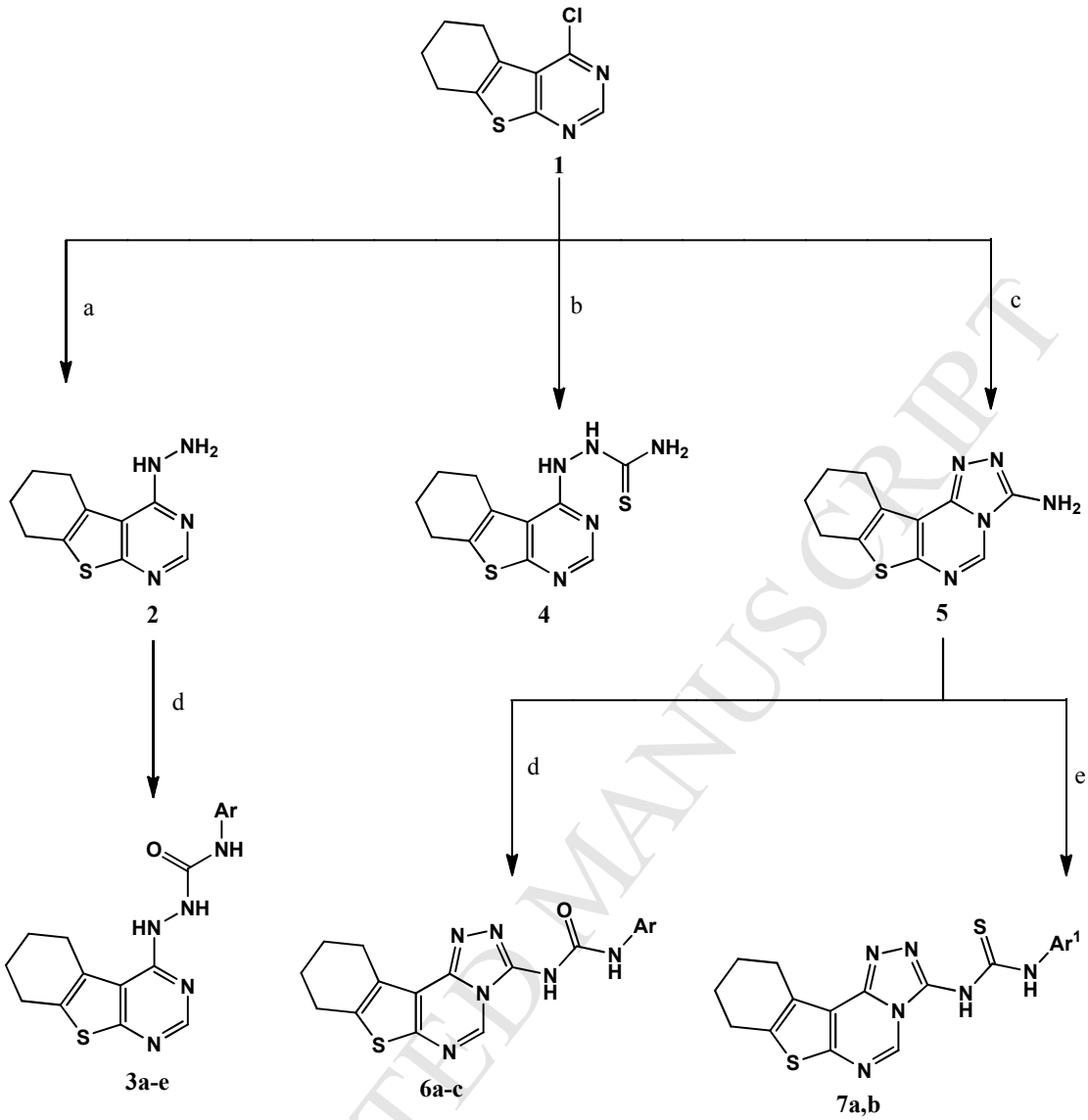

Scheme 1. The synthetic path and reagents for the preparation of the target compounds **2-7**.

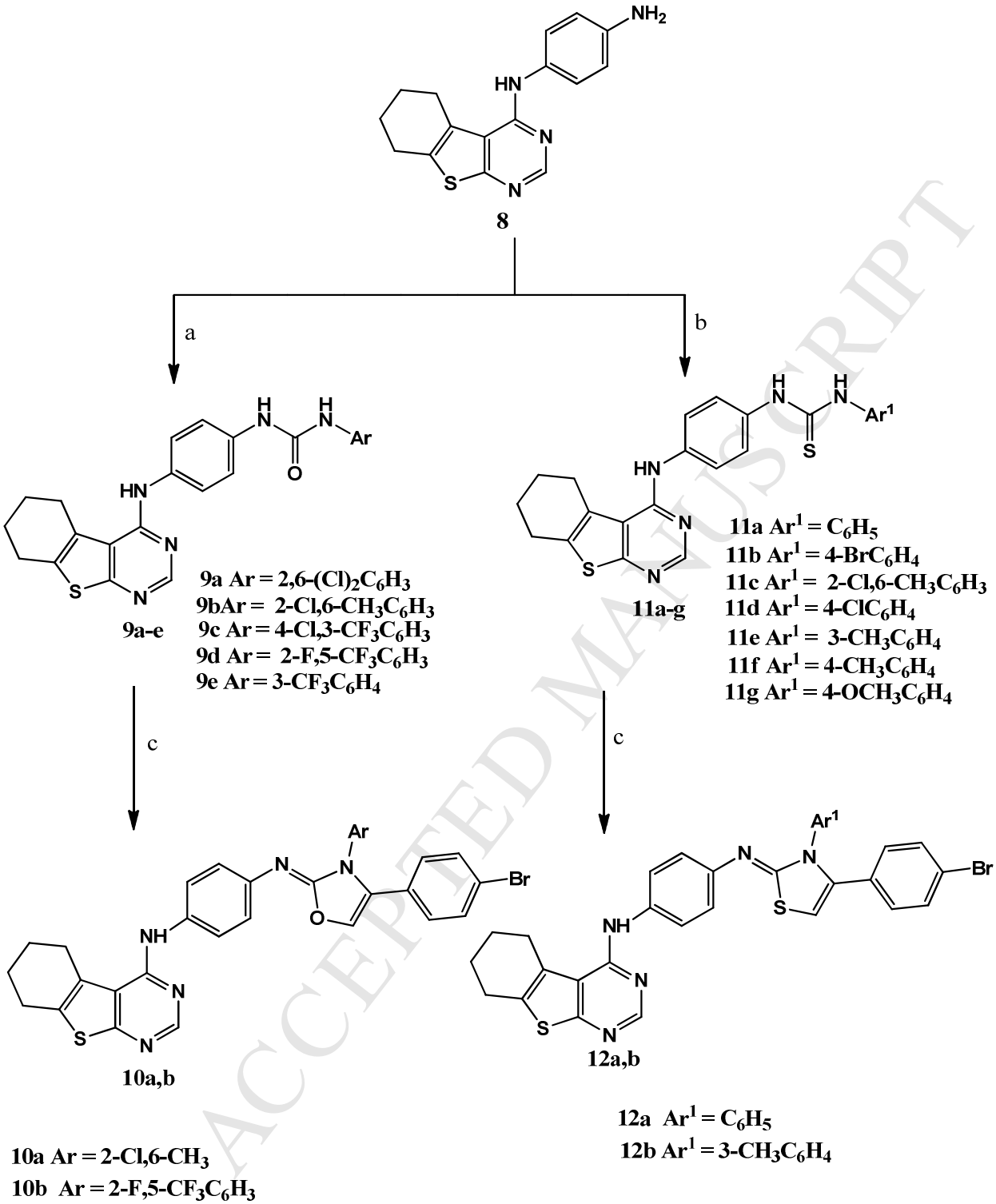

Reagents and conditions: a) ArNCO, CH_2Cl_2, 0°C;

b) Ar^1NCS, K_2CO_3, dioxane, reflux 12h;

c) 4-Bromophenacyl bromide, $NaCOOCH_3$, C_2H_5OH, reflux 6h

Scheme 2. The synthetic path and reagents for the preparation of the target compounds **9-12**.

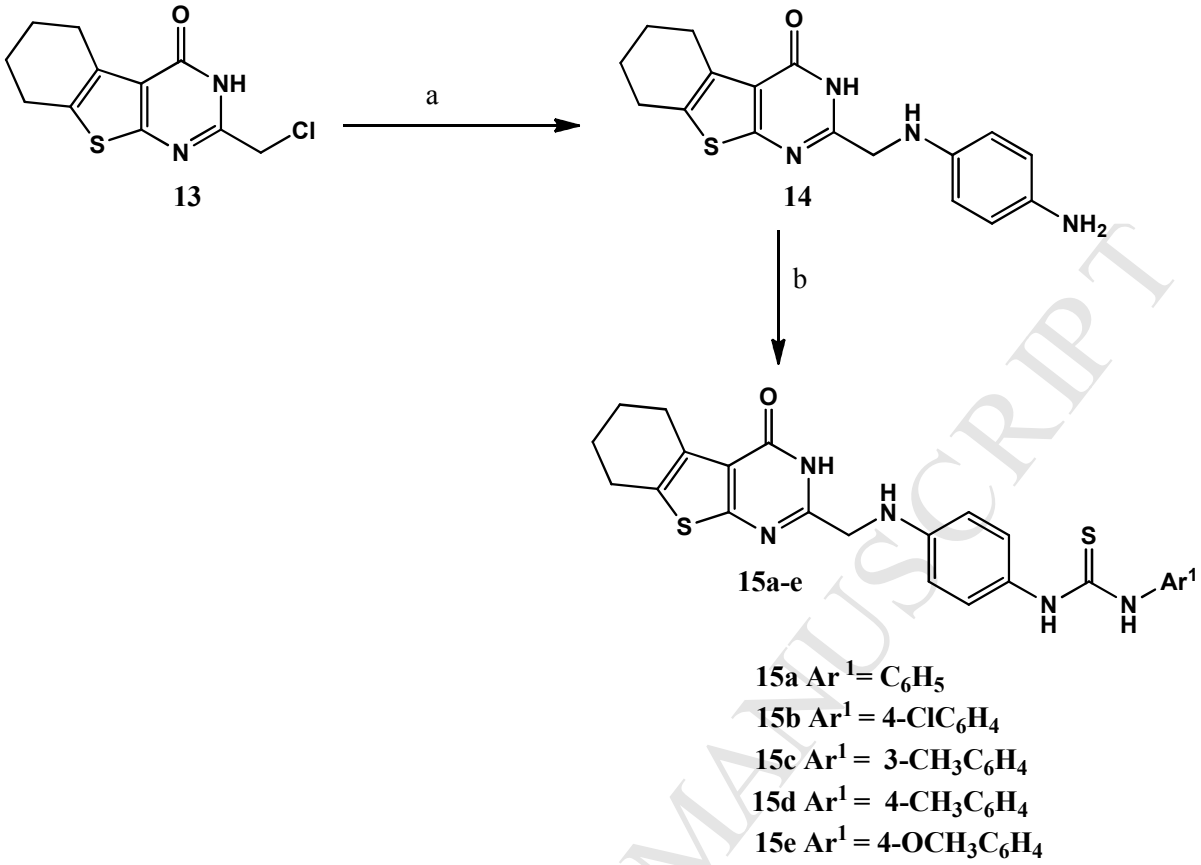

15a Ar ^{1}= C_6H_5
15b Ar^1 = 4-ClC_6H_4
15c Ar^1 = 3-$CH_3C_6H_4$
15d Ar^1 = 4-$CH_3C_6H_4$
15e Ar^1 = 4-$OCH_3C_6H_4$

Reagents and conditions: a) p-Phenylenediamine, TEA, C_2H_5OH, reflux 15h;
b) Ar^1NCS, K_2CO_3, dioxane, reflux 25h.

Scheme 3. The synthetic path and reagents for the preparation of the target compounds **14**, **15**.

- A series of new thieno[2,3-d]pyrimidines were synthesized.
- The anticancer activity of the new compounds were tested *in vitro*.
- Multi-sited enzyme small molecule inhibitor **9c** was identified.
- Compound **9c** showed IC_{50}= 9.29 µM against topo II and induced p53 mediated apoptosis.
- Compound **9c** exhibited IC_{50}= 0.2 µM against VEGFR-2.